Project Number: GSF MQP M101

PNEUMATIC ACTUATOR DEVELOPMENT FOR MRI ROBOTS

A Major Qualifying Project Report
Submitted to the Faculty
of the
WORCESTER POLYTECHNIC INSTITUTE
in partial fulfillment of the requirements for
the Degree of Bachelor of Science
in Mechanical Engineering
Robotics Engineering
Electrical and Computer Engineering
by

_____

Michael DiBlasi

_____

Andrew Nehring

_____

Andrew Smith

Date: 4/ 29/ 2010

Approved:

Keywords:

1. Pneumatics
2. Hydraulics
3. MRI
4. Robot
5. Stepper motor

_____

Prof. Greg Fischer, Major Advisor

_____

Prof. Taskin Padir, Co-Advisor

Acknowledgements

We would like to thank the amazing support of the entire WPI community, but a few groups stand apart in the realization of this project. This project would not have been possible without them. Professor Greg Fischer and Taskin Padir shared their knowledge, support and love for the material topics in ways that will last outside the bounds of this project. The AIM Lab at WPI gave the group materials, funds and work space necessary in completing the project goals. National Instruments was instrumental in its contribution of the cRIO Hardware platform as well as the LabVIEW software licenses and system support. Michael Fagan ’11 committed hours of manufacturing reference and experience as did both Daniel Jones ‘11 and Daniel Cullen ’10 for electrical and programming support. This project would not have been possible without the combined efforts of these thoughtful and knowledgeable individuals and generous contributions of the aforementioned sponsors.

Abstract

Magnetic Resonance Imaging (MRI) is an excellent imaging modality for many conditions, but to date there has been limited success in harnessing this modality for the guidance of interventional procedures. To aid in the development of interventional devices for MRI, the modular linear hybrid pneumatic-hydraulic MRI robot actuator was designed. It is a modular solution to precision motion in a medical MRI environment. The implementation of this electronics free, non-ferrous and nearly completely non-metallic linear driver mechanism may be configured to give a clinician the ability to place needles, electrodes, grippers, sensors, syringes or other medical instruments with an extraordinary level of flexibility and precision. Its modular design allows for rapid prototyping of robotic systems and paves the way for more advanced and complex minimally invasive procedures under real-time MRI guidance. The team's design will be used as a platform for future MRI robot designs and research in collaboration with the UMass Medical School.

Table of Contents

List of Figures

Authorship

ACKNOWLEDGEMENTS	**MD**
ABSTRACT	**MD**
TABLE OF CONTENTS	
LIST OF TABLES	
LIST OF FIGURES	
AUTHORSHIP	
INTRODUCTION	**MD**
BACKGROUND RESEARCH	**MD, AN**
METHODOLOGY	**AN, AS**
VALIDATION	**AN, AS**
DISCUSSION	**AN, AS**
FUTURE WORKS	**MD, AN, AS**
WORKS CITED	**MD, AN**
APPENDICES	**AN. AS**

Introduction

Magnetic resonance imaging (MRI) technology, since its inception in 1972[1], has allowed for an incredibly detailed view of the soft in the human body[2]. MRI scanning is used as a diagnostic tool for discerning abnormal tissue from healthy for conditions such as organ infections, tumors and heart complications. Unfortunately due to the intricacies around human safety and MRI compatibility it still remains largely disconnected from direct use in guiding medical procedures. Procedural accuracy, repeatability and speed are fundamental in the field of medicine and can mean the difference between life and death.

Over the years, robots have continued their transition from science fiction and the surreal into real world applications. MRI compatible robots hold an incredible potential to revolutionize the medical field and bring MRI scanning technology into the Operating Room (OR), or rather, bring the OR into the MRI. Robotic surgical assistants, though still a maturing development, are becoming the next step in robotic assistance as well as human-robot interface technologies.[3]

An MRI compliant surgical robot would enable operators an unprecedented level of medical unity and could one day even integrate an automated feedback system with the MRI scanners in real-time. Research into, and development of precision linear motion

---

[1] Principles of Magnetic Resonance Imaging, Page 2
[2] Magnetic Resonance Imaging, Page 1
[3] Ergonomic evaluation and guidelines for use of the daVinci Robot System

techniques in a medical MRI environment could lead to virtually limitless applications in the future of medicinal technology.

Background Research

Introduction to MRI

NMR (Nuclear Magnetic Resonance) is the condition in which the nuclei of atoms react to the combination of static and oscillating magnetic fields. This response is used in order to determine physical, chemical and even biological properties of matter. NMR spectroscopy scales from one to three-dimensional analysis depending on the structure intricacy. While solid state spectroscopy can be appropriately used to determine solid and liquid structures, dynamic images can also be obtained through similar techniques.[4]The name change from NMR to MRI when referring to medical imaging using the technology comes from the publics' fear of the word 'nuclear' since magnetic resonance is a much less intimidating name.

The principles of NMR were first characterized in 1946 by Felix Bloch at Stanford and Edward Mills Purcell of Harvard for fluids and solids respectively. The 1952 Nobel Prize in Physics went to the pair for introducing the technique that would allow for MRI to become a reality.[5]

An MRI machine, shown in Figure 1[6] uses the properties of NMR to determine the properties and state of the scanned item based on its response to magnetic fields. Through

[4] The Basics of NMR
[5] Magnetic Resonance Imaging: Basic Principles, Page 23
[6] http://miriam-english.org/files/images/standard-MRI-machine.jpg

the use of a standing and oscillating magnetic field, the responses can be measured and compared against known materials and their responses. The raw data is typically represented as a grayscale image, in either two or three dimensions depending on the specific type of scan being done, some sample images can be seen in Figure 2[7].

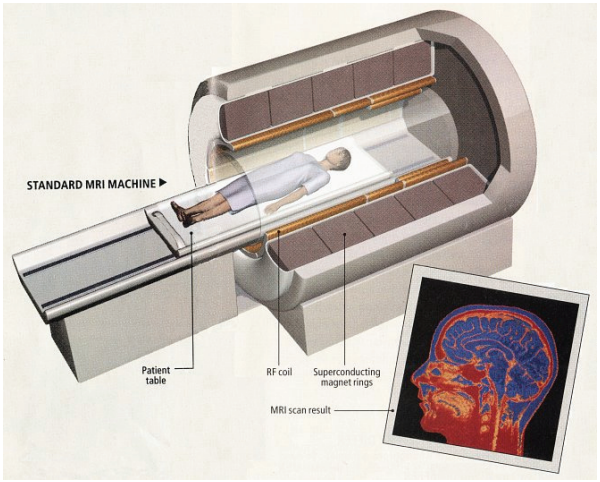

Figure 1 – A Modern MRI Machine

Because of the multiple parametric nature of MRI, there are a number of scanning techniques. Repetition Time (TR) variable adjusts the two periods of RF-pulse excitation and emission, heavily influencing image quality. Echo Time (TE) represents the millisecond time scan periods to accurately map intricate structures. Some materials responses are extremely short and must be accounted for in order to appropriately represent it.[8]

Figure 2 - MRI Sample Images

[7] http://science.nationalgeographic.com/staticfiles/NGS/Shared/StaticFiles/Science/Images/Content/brain-mri-cb060962-sw.jpg
[8] Magnetic Resonance Imaging: Basic Principles, Page 81

A Radio Frequency (RF) pulse is another name for the oscillating electric field that is used to excite the protons in hydrogen atoms and cause them to resonate. This pulse is enabled on the microsecond scale, and is generated in conjunction with time varying magnetic fields that are considerably weaker than the static magnetic field and used for slice location selection and image construction.[9]

When putting objects in or near the MRI scanner, a magnetic field may be created by an electric current running through a strand or coil of wire that can disrupt the scanners field. Similarly, it is affected by metallic conductors that induce eddy currents and ferrous materials that directly distort the field. The resulting influences from the metallic objects in the scanner bore alter the magnetic field (Field Homogeneity) which will profoundly distort the received image.[10] These factors are covered in-depth in the MRI Compatibility section.

[9] Principles of Magnetic Resonance Imaging, Page 70
[10] Essentials of Electromagnetics for Engineering, Page 271

MRI Applications

MRI scans are typically patient safe as they use non-ionizing radiation, unlike CT scans and X-rays. MRI scans can be of extremely high quality, with sub-millimeter and true three-dimensional scan capabilities in real-time. MRI technology specifically targets soft tissue and is optimized for such materials. Because of these high quality technical specifications, MRI technology is ideal for guiding biopsies, surgical procedures and virtually every kind of medical operation. MRI examinations are often used to identify tumors, blood vessel blockages, specific organ diseases and infections and even to measure brain activity. Different conditions and physical states of tissue can be interpreted from MRI scans, allowing doctors to differentiate sick and healthy cells that appear as grayscale images. MRI machines are considered indispensable as modern diagnostic aids.

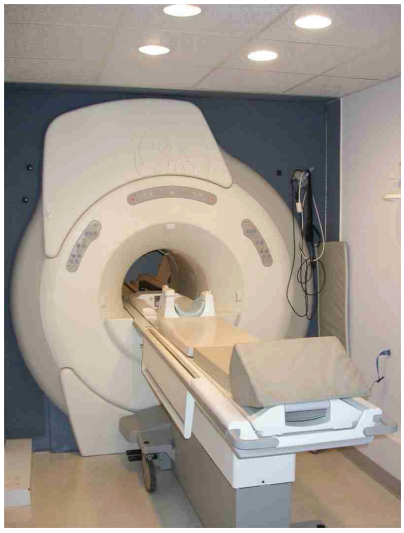

Figure 3 - Closed MRI

Figure 4 - Open MRI

There are two main types of MRI machines used in hospitals. A traditional high-field closed MRI machine, shown in Figure 3[11], has more accurate imaging capabilities but is more constrained for affecting patient access and can cause claustrophobia. In the closed machine the magnetic coil goes completely around the patient, which is that cause for the more accurate yet tighter scanning areas. Physicians tend to use the closed model for the accuracy benefits. An open MRI, shown in Figure 4[12], has, as the name implies, a more open and larger work area but does not have as accurate imaging as the closed type due to the lower field strengths and poorer magnetic field homogeneity. The open style typically allows for heavier patients (up to 450 pounds).

A relatively new style of MRI equipment is a standing model. This hardware permits physicians to examine patients in the standing position allowing for the view of weight bearing forces.[13] It may be more accurate in scanning for spinal conditions but result in more pain for the patient, assuming they can get into the required position at all. As with the open scanner, field strength is weaker and these scanners are usually restricted in their ability to do general imaging of the body.

Since open MRIs are less common and provide lower quality images, the focus of our work is on developing a system that will enable the use of readily available diagnostic scanners to help guide interventional procedures.

---

[11] http://www.rajabgroup.com/Images/Superstar%200.35T%20Open%20MRI%20n.JPG
[12] http://www.mritoday.net/MRI2.JPG
[13] Open Stand-Up MRI: A New Instrument for Positional Neuroimaging

MRI Compatibility

Image artifacts come from a number of sources, including noise from wiring entering the scanner room, unstable power supplies and uncalibrated hardware, and also from distortion due to metals or ferrous materials. In addition to the obvious safety concerns, ferrous materials can cause inhomogeneities in the scanning magnetic field. Random RF noise causes static-like artifacts in the images, samples of which are shown in Figure 5.

The important types of MRI interference include distortion and noise. Distortion interference is the condition where the image is stretched or distorted, or may present itself as large signal voids in the image. Electrical noise in the system creates static in the image, much like bad reception on an analog TV and stems from the scanner's receiver antenna picking up stray signals during imaging. Analog signals with jumps or spikes in the waveform are an example of this kind of electrical noise. These types of interference can prove to be extremely problematic in such a precise and delicate operation and if not appropriately considered and dealt

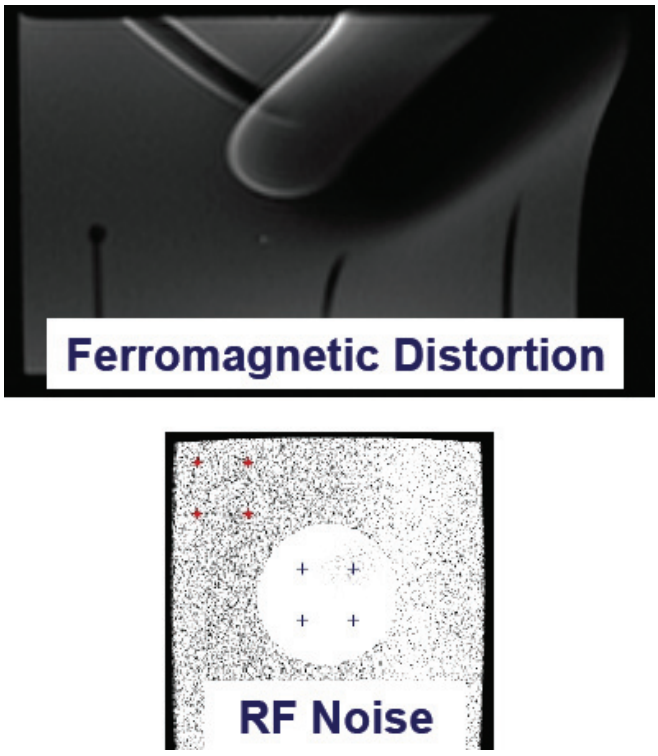

Figure 5 - Sample Distortion

with, they can cause problems such as false diagnoses.

Pacemakers, dental implants and orthopedic hardware such as screws and plates cause severe interference in MRI scans that may range from a small signal void to image distortion to a major safety hazard. Future iterations of these products are striving for MRI compatibility. Patients with these conditions are often strongly recommended to try other imaging techniques as besides interfering with the machinery, the items can malfunction or overheat.

Ultrasonic motors are electric motors that are powered through the ultrasonic vibration of a stator and behave similarly to piezoelectric motors. Unlike piezoelectric motors, ultrasonic drivers use resonance and high frequency vibration to control the rotor. These motors are common among camera autofocus drivers because of their high speeds and quiet operation. Figure 6[14] shows the influence of each motion device on signal to noise ratio (SNR) on a test scan of a 1.5 Tesla MRI, with the

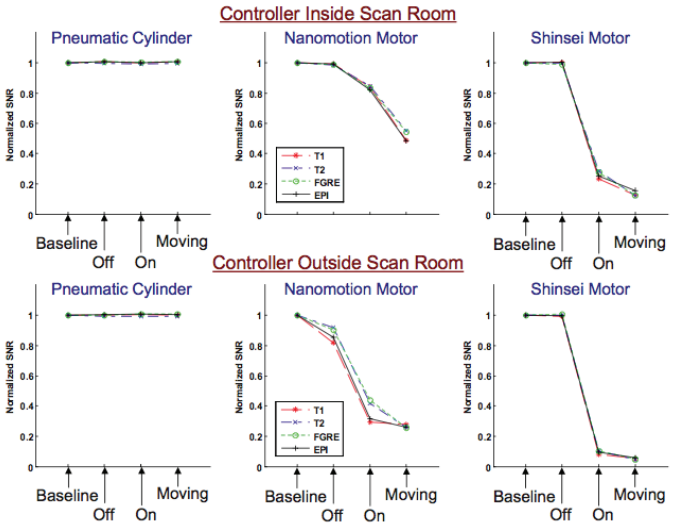

Figure 6 - Actuator Distortion

[14] Fischer, Greg, Axel Krieger, Iulian Iordachita, Csaba Csoma, Louis Whitcomb, and Gabor Fichtinger. "MRI Compatibility of Robot Actuation Techniques – A Comparative Study." *MICCAI 2008*. Web.

controller both inside and outside of the scanning room. When compared with a pneumatic cylinder, pneumatics had no visible effect on the SNR even when running, while the piezoelectric motor (Nanomotion motor) had a small decrease in SNR under rest, but considerable negative effect on the noise levels when enabled. The ultrasonic motor (Shinsei motor) produced no change in SNR until it was turned on, where it caused the most significant drop in the ratio level. In terms of minimizing noise in the image, pneumatic controllers and drivers are the most effective.

Piezoelectric motors can be used in MRI environments if they are designed appropriately and not run simultaneously with the scanning equipment.[15] Piezoelectric motors are driven through the use of an electric field, translating ultrasonic vibrations into linear or rotary motion. Ceramic drivers allow these particular motors to cater to the material constraints of the MRI environment but the inclusion of electric field control forces the device to remain off during scans.

Strong electric currents and metals can cause interference with the magnetic fields of the machine, resulting in noise in the imaging or even damaged equipment from attracted materials. Metals with even small amounts of ferromagnetic elements can cause trouble in a magnetic field the size of an MRI machine. All metals are conductive and will cause an effect on the image to some degree but particular types and shapes can cause much more damage.

[15] Implantable linear motor is made of piezoceramics for MRI

Existing Solutions

The medical environment is the perfect place for robotic applications because of the high levels of precision and repeatability. The benefits of such robotically controlled and assisted systems continue to grow daily. The daVinci surgical robot[16] is the most popular surgical robot on the market today. The daVinci is capable of assisting surgeons in laparoscopic procedures with a wide array of benefits. Robots by nature are more precise and repeatable than humans and allow for corrective software and optimized hardware to go above and beyond what humans alone can achieve. The miniaturization of tooling, 3-dimensional cameras and increased dexterity allow for many secondary benefits. Less blood loss from smaller wounds means shorter healing times and less pain and scarring as well as decreased chances of complications.

The design of MRI compatible motion techniques may one day allow all of the benefits of medical robotics to be combined with the high precision real time MRI scanning feedback system. Brigham Hospital developed one of the first MRI compatible robotic manipulators for tool placement,

Figure 7 - Brigham and Women's MRI Robot

[16] MRI-guided laparoscopic and robotic surgery for malignancies

shown in Figure 7[17]. It was specifically designed to hold a catheter to assist a surgeon. Although physically possible to insert the catheter, it was deemed ethical and legally dangerous. This device acts as a simple proof of concept of MRI compatible robots and a stepping stone for more advanced systems.

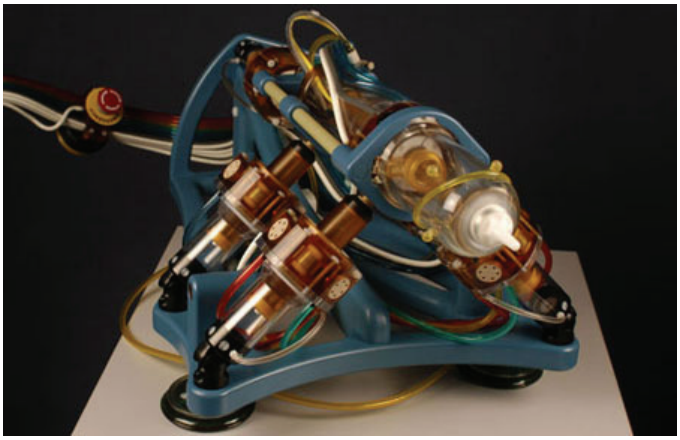

Figure 8 - MrBot Design

MrBot, shown in Figure 8, was developed by the Johns Hopkins Urology Robotics Lab in April of 2007 for MRI-guided biopsies[18]. The device was designed entirely of ceramic, plastic and rubber and obtains 5 degrees-of-freedom from six pneumatic drivers and a gear set as a driving force. The developers claim to have smooth motion in steps as small as 50 micrometers, but overall needle tip precision of 1 millimeter in 3d space.

Since typical MRI machines have a resolution of up to 0.1 millimeters in diagnostic imaging, this device could benefit from an increase in its own precision. The pneumatic drivers operate directly from the pressurized air line from the control system and can achieve steps as small as 0.55 millimeters[19]. By regulating the pneumatic pressure on

---

[17] Surgical assist robot for the active navigation in the intraoperative MRI: Hardware design issues

[18] Magnetic Resonance Imaging Compatible Robotic System for Fully Automated Brachytherapy Seed Placement

[19] Motion control of pneumatic drives

either side of the cylinder it can achieve motion and locking functionality. Because they are directly driven by hospital provided air they lack the necessary forces and reliability that would be required for a procedure to be carried out safely on a patient. Since air regulators can be unreliable the system could fail due to a brown-out or fluctuation in air pressure. Although MRI compatibility is a very important aspect of these robotic devices safety still comes first. Besides the plunger itself, the system contains no linear sliders, instead using the pneumatic cylinders as joints for the system in general. Because of the way the system handles motion, it is based around a central point and has a very limited adjustment range.

The device is quite large relative to the patient platform bed, forcing the user onto their side, as seen in Figure 9. Patients tend to lie on their backs during MRI procedures and standard operations because of organ shift. Organ placement becomes unpredictable in other orientations which make surgeries and scanning techniques difficult if not impossible. MRI scans sometimes take over 15 minutes to complete, and optimal images require the patient to stay nearly perfectly still. Patients are often lightly restrained to help reduce shift but laying on their side introduces a new set of complexities in ergonomics and comfort.

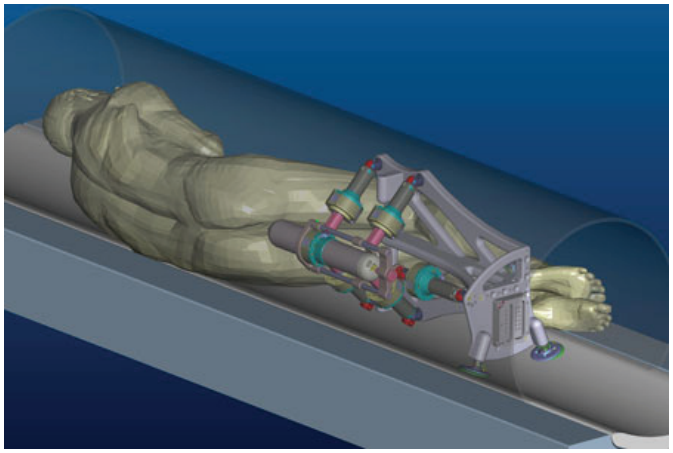

Figure 9 - MrBot application

The Stereotactic Neural Intervention Unit, shown in Figure 10, was designed by the AIM Lab at WPI in 2009 and allows for the accurate placement of a needle and rotation around the specified point using linkages. The system uses piezoelectric motors which

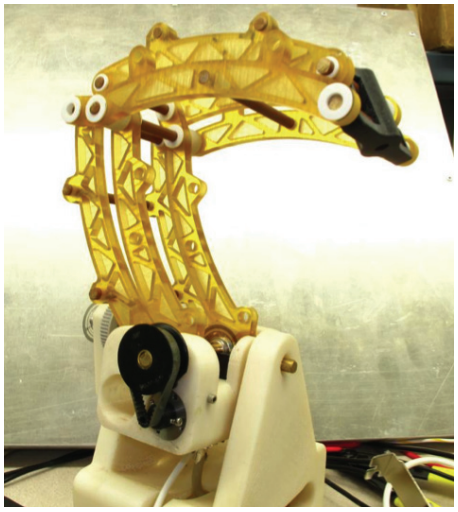

Figure 10 - Stereotactic Neural Intervention Unit

were shown to be MRI compatible with custom drive circuitry, however it would clearly be beneficial if we could develop a system with absolutely no electronics on board[20]. Similar to the MrBot, this system does not have a large range of motion, as it was designed for motion to and rotation around a point in 3-D space. The device is useful in particular closed loop systems but is not modular enough to adapt to a changing environment, and could benefit from linear placement.

Elhawary's 1-DOF actuated linear robotic platform, shown in Figure 11, utilizes piezoelectric motors for motion in an MRI environment.[21] The system is accurate to within 0.1 millimeters and contains integrated position sensors for closed loop position control. It is undesirable to use piezoelectric motion because of the drawbacks inherent in its usage in MRI applications. Pneumatic actuation offers a smaller

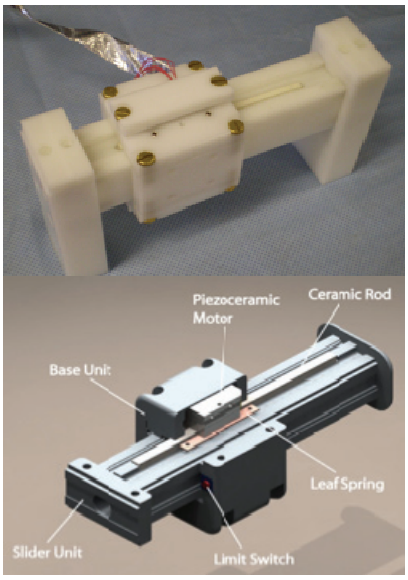

Figure 11 - Elhawary's Piezoelectric Modular Actuator

[20] MRI Compatibility Evaluation of a Piezoelectric Actuator System for a Neural Interventional Robot

[21] A Modular Approach to MRI Compatible Robotics: Interconnectable One DOF stages

impact on image quality than all other MRI compatible motion systems in use today.

The University of Calgary's NeuroArm, Figure 12, design achieves high levels of precision in 6 DOF using piezoelectric rotational drivers.[22] Ceramic piezoelectric motors drive fingers in the drive system in order to achieve 25 microns of precision. This design sacrifices for MRI compatibility for precision, and can be grouped with the other piezoelectric systems. The pulse width modulation (PWM) electronic signals will still interfere with image quality and remain behind the optimal choice of pneumatics.

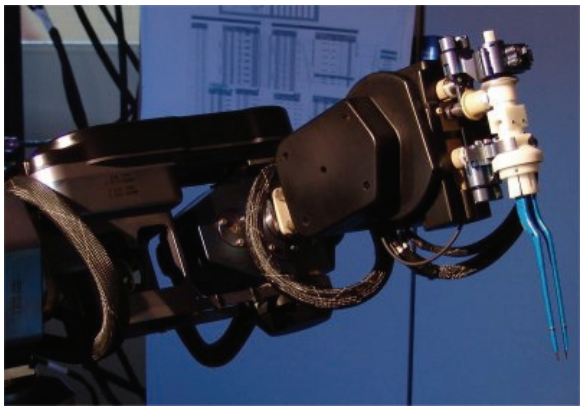

Figure 12 - University of Calgary NeuroArm

Figure 13 - Innomotion Arm

The Innomotion project, shown in Figure 13, from the University of Dundee in Scotland utilized pneumatics for its 6 DOF robotic arm, and designed specifically for Percutaneous applications[23]. Unfortunately

[22] World's first nonmagnetic robot arm.
[23] INNOMOTION for Percutaneous Image-Guided Interventions

the system is not particularly precise, deviating up to 1 millimeter from the targeted area. Although pneumatics are able to operate within an MRI machine without compromising the readings it is another challenge to create the system to be accurate and repeatable enough for medical use.

Comparing the types of motion and their effects on image quality makes it clear that a pneumatics based system is the optimal solution. Combining the modularity and closed control feedback of the linear actuators with the precision of the pneumatic stepper design should allow for surgical quality motion without sacrificing MRI scan quality. By integrating the systems into a single, solid design the base for an MRI general service or even surgical robot can come to fruition.

Methodology

Project Scope

The background research into this project showed two major problems to overcome. To begin with, servo controlled pneumatically controlled systems don't reliably run with ththe nevessary resolution. Most pneumatic systems are fully extended or fully retracted, with a couple of patents and production models capable of a centered position as well. Attempts at servo controlled pneumatics often are only successful in well modeled, static environments and do not adapt well to the changing environment or load that would be present in a medical application. The over 1000 steps needed for this mechanism would be a huge step forward in pneumatic technology.

While this problem would certainly be challenge enough, the finished product also needed to be MRI-compatible. Discussed in more detail in the background section, this essentially means that there can be no ferrous metals whatsoever, no large pieces of any conductive material, and no electrical components. With this severe restriction imposed on the complexity of solving the resolution problem inherent in pneumatic systems, the possible solutions are very limited.

These actuators will be used to create multiple degree of freedom systems, sometimes with different requirements for each axis of motion. As such, the actuators should be designed to be modular for internally and externally. The system should be able to be modified to give different output characteristics such as force and travel, while keeping the form factor small enough and standardized to allow for multiple actuators to be stacked to create complex systems.

Design Specifications

Quantitative

- Minimum of 15.3 centimeters (6 inches) of end-to-end travel
- Uniquely measurable 0.1 millimeter (0.004 inch) mechanical steps
- At least 20 Newtons (4.5 pound-force) output
- End-to-end travel in 15 seconds
- Control system must be able to run six actuators

Qualitative:

- Mechanism must be able to lock, and the fail-safe state should do so automatically if a pressure loss occurs.
- Manual mode should be included to allow the operator to slide the mechanism to the proper location. Step increments must resume without jumps.
- Compact size.
- Easy to interface with duplicates to create multiple degree of freedom machines.
- Full MRI-Compatibility:
    - No ferrous metals
    - No large conductive parts, MRI Machine image should not be noticeably distorted
    - No on-board electronics for drive and sensing.
- Cable running from machine should be small and robust carry only air lines and fiber optic cables.
- Mechanism's motions to create forward and backward steps should be unique to ensure predictable output.
- Mechanism must be scalable in force, range, and step size.
- System must be closed loop, with integrated joint position sensing.

Design Specifications Discussion

The design requirements are all based on what the machine will be accomplishing in a surgical environment. Six inches of translation in every axis will allow the mechanism to be used in a table system (i.e. no motion amplification) while being able to access the full area of most common surgeries, although so long as the machine is scalable, this requirement is not too strict. The resolution of modern MRI machines varies due to the scan parameters used, but is rarely at or below 0.1 millimeters in typical diagnostic imaging scenarios. The force needed to insert a tool into a prostate sets the force output at 20 Newtons[24], which also allows for a reasonable margin of safety on other organs, which are generally less robust.

While the actuator might be used in any size system, six degrees of freedom (DOF) is the minimum required to access every point in a manipulator's workspace (including both translational and rotational axes). This flexibility can prove crucial in surgery, allowing the operator to work around other organs and work below the skin in minimally invasive procedures. To keep this use of the mechanism practical, the control system should be easily expandable to six of the actuators. However, the mechanism may also be used as a 3-DOF translational base for more application-specific end effectors such as the neuro robot discussed earlier or combined with other actuators when integrated into a complete

[24] "Robot-assisted prostate brachytherapy"

system. The final quantitative requirement is the 15 second end-to-end travel time. Since rapid motions are not required, and in fact undesirable, in surgery, this was chosen as a reasonable time to traverse the full range of motion. This also makes it the least critical of the quantitative requirements, while the resolution and accuracy of the machine are by far the most important.

Several of the qualitative requirements are based in safety. For example, should a pressure loss occur, the driving mechanism of the system could become unpredictable, or simply stop providing an input to the system. In this case, whatever is being used on the end of the manipulator could drop or move on its own, possibly with severe repercussions during surgery. To prevent this, the system must be designed so that the fail-safe state is to lock and prevent motion without manual intervention in the event of a system pressure loss.

Working in an MRI environment also places severe conditions on the design of any mechanism. As discussed in the background, this means that no ferrous metals can be used in the design, and neither can any large pieces of a conductive material. Ferrous metals would be turned into projectiles by the powerful magnetic fields inside of the MRI, and conductive materials would have current induced in them, which would warp the image generated by the MRI. Both of these, especially the former, cannot be allowed to occur.

General Design Decisions

The first step in created the actuator was to choose a basic concept. The only precedent for a pneumatic stepping actuator in an MRI environment was the motor included in the MrBOT from Johns Hopkins[25], but this was a bulky, inaccurate mechanism based rotary harmonic motion, which is too fragile for the scale and accuracy that needed in this new mechanism. There is also the modular linear stepping actuator from the Imperial College London[26], but this uses piezoelectric actuators to provide the motion, and removing all electronic components from the machine would be highly desirable. The design developed in this project is a pneumatic-hydraulic hybrid actuator, an improvement on current technology in its accuracy and force capabilities, as well as being simpler and capable of being far more compact.

At the beginning of the project work there were many different concepts for how to proceed. To determine the final design choice, a design matrix was used as it is described below.

The first design, presented by Professor Fischer, consisted of several actuated fingers and a rack gear used to create a linear harmonic motor. This worked by having the finger spacing offset from the pitch of the rack gear, so that as the fingers fire in order, the

[25] Magnetic Resonance Imaging Compatible Robotic System for Fully Automated Brachytherapy Seed Placement
[26] A Modular Approach to MRI Compatible Robotics: Interconnectable One DOF stages

rack gear would progress slowly forward. In this way, a large, inaccurate motion could be converted a movement of the precision needed for the final mechanism.

The next design considered used pneumatic pistons to turn a crankshaft, in precise angular displacements. A gear train would be used to reduce these angular displacements, before finally advancing a rack gear by that precise motion. There was a major flaw in this design however, with plastic gears and plastic mountings, there would be a substantial amount of backlash in the system. This is highly undesirable in this system, as any slop in the mechanism could have serious repercussions in a surgical environment.

A linkage driven solution was also considered. Although the details of this method were never fully worked out, the concept consisted of using pneumatics to turn the crank of a four-bar linkage. This, in turn, would move into a rack gear, engage, and move it forward similar to the method of the finger walking mechanism. However, by tweaking the linkage, much higher efficiencies can be achieved.

Kevin Harrington presented another solution using a mechanism similar to a watch escapement. By applying pressure to an output, a rotational mass-spring system could be used to only allow forward motion in precisely timed steps. By carefully monitoring the time and turning the pressure off at the right time, a precise motion could be achieved.

The final design option was presented by Greg Cole. This system is a pneumatic-hydraulic hybrid system, where pneumatic valves and a pneumatic pump control the motion of hydraulic fluid, which is used to give the precision needed at the final output. If the volumes could be worked out to have one pump motion move the output stage by the desired resolution, system control would be very simple.

With these ideas in place, the next step was to use a decision matrix, shown in Figure 14, to cut down the options to a single design to pursue further. The crankshaft design was thrown out due to the critical problem with gear backlash, as this would doom the concept and may not show up in the design matrix, destroying the validity of the matrix. The finger, linkage, escapement, and hydraulic systems were all put into the matrix.

The categories that were determined to be the most important for the finished product were controllability, reliability, speed, efficiency, and simplicity. The controllability metric measures how easy it is maintain an accurate system output and ensure system stability. Reliability is a measurement of how simple it will be to ensure that the mechanism will not break down during operation, and if it does, how easy it will be to fix. Speed and efficiency metrics are based off of the capability of the mechanism to move quickly and without wasting energy, and the simplicity metric measures how much time it will take to design the machine.

These categories were then weighted according to their relative importance. Controllability is the most important metric in determining the system, while simplicity issues

	Multiplier	Fingers	Linkage	Escapement	Hydraulic
Control	10	10	6	6	10
Reliability	8	8	7	6	10
Speed	7	3	5	10	8
Efficiency	7	1	5	7	10
Simplicity	5	10	7	3	5
		242	**221**	**242**	**331**

Figure 14 - Decision Matrix

can be overcome. Reliability, speed, and efficiency are all approximately the same, as these too can be overcome with proper design, although this is a more challenging problem to overcome with detailed design.

The different designs were then reviewed with special attention paid to the qualities that were considered important for the project. Each design was assigned a value between 1 and 10 in each category. The sum of these values, taking into account their respective multipliers, sum to find the designs' totals, the highest of which signifies the best option. Based off of the decision matrix arrived at during brainstorming, the hydraulic hybrid design is the best option.

Methods

Overall System Layout

To reiterate the design in more detail, the system being prototyped is a closed hydraulic system controlled by pneumatic inputs. The control system handles the pneumatic system which both creates and directs the flow of hydraulic fluid. The hydraulic fluid is pumped through a valve system to determine the direction of motion, and into a large driven piston. The change in diameter between the pump and driven pistons allows for the hydraulic system to have two major advantages: 1) decreasing the linear displacements (i.e. improved accuracy) between the pump and the output, and 2) increasing the force substantially (i.e. force amplification). The position of the output stage is then read by an integrated fiber optic absolute encoder, which turns the mechanism into a closed loop system and ensures output accuracy. This system is summarized as a block diagram in Figure 15.

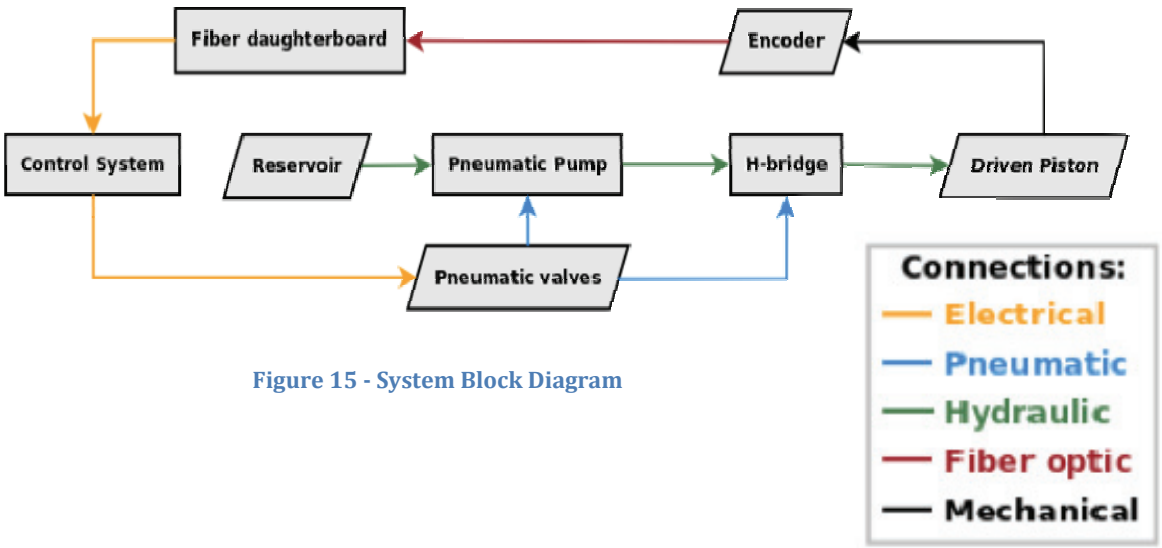

Figure 15 - System Block Diagram

Controller

The controller for the system will be the National Instruments (NI) CompactRIO, shown in Figure 16. This consists of a chassis module containing the main processor, as well as a Field-Programmable Gate Array (FPGA) to handle signal processing from the input/output modules. The chassis can hold up to eight of these modules, and there is a wide range of options for these. For this application, digital I/O, both high power (pneumatic solenoids) and low power (digital signals) are the most critical, although analog sensors may be added in the future. For these reasons, the chassis was equipped with a mix of digital and analog I/O modules. This high level of modularity is an excellent fit for this application, allowing the end user to adjust the mix of modules to fit even more modules, or add more analog sensor capabilities.

Figure 16 - A NI cRIO

The NI CompactRIO is also designed to operate with NI LabVIEW, a graphical programming language. This language is designed to create a graphical user interface (GUI) with hardware interaction provided by a block diagram program running in the background. As a simple GUI would be a great asset for allowing users with minimal technical training to operate the actuator, this is another excellent asset for the project.

Pneumatic-Hydraulic System

The NI CompactRIO is connected to an array of six pneumatic valves, shown in Figure 17. This would provide plenty of independent channels for whatever valve system was designed, although the number of channels needed should be substantially fewer. Any

valve system designed should not need more than four lines, as the final mechanism needs only four modes (forward, backward, locked, and coast). If we ran over this limit, the CompactRIO would not be able to control enough of the actuators to meet our modularity target, so setting the limit at an early stage would help to ensure that this goal is met.

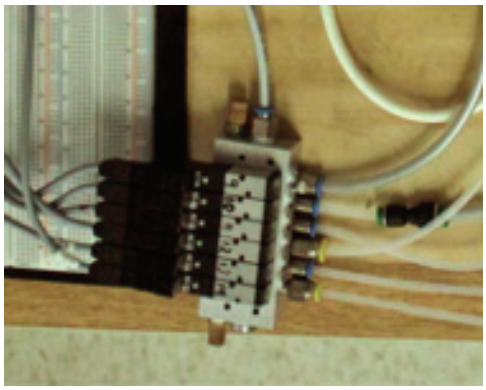

Figure 17 - Prototype Solenoids

The pump for this actuator needs to move a very small amount of hydraulic fluid through the system with each pneumatic input. The pump would be a single acting input to a double acting piston. What this means, is that the pneumatic input to the system is turned on to move the piston one direction, and a spring return pushed the piston back when the pressure is released. The piston, however, is drawing in fluid on one side and pushing it out the other as it moves in either direction. A check valve system is required to ensure that the fluid is moving in the proper direction, but this is a well established hydraulic system, although the pneumatic input is relatively novel.

The driven piston is nothing more than a double acting hydraulic piston. As fluid is pumped into one side, the piston moves and pushed fluid back out of the other. This, along with the double acting motion of the pump, keeps the hydraulic system volume theoretically constant, reducing the need for a large hydraulic reservoir to absorb volume fluctuations.

The concept of the pump and the driven pistons is relatively simple, but the valve design is much more difficult. This was by far the most complex part of the entire project, as it needed to control four different system modes with no more than four inputs while

remaining compact. This sort of system is generally done in hydraulics by using a multiple position manual switch, which the operator will put into whatever mode they need. Automatically controlled hydraulics rarely use more than off/on control, or simply switch which side of a system the pressure is being applied to, and allow the low pressure fluid to find its way back to the reservoir through uncontrolled paths. This was completely unacceptable in this situation, as locking and coasting modes were needed as well, and there was no simple way to create a four position pneumatic to control a multiple position switch.

DC electric motors need this same kind of control, however, and the H-Bridge circuit is used extensively to drive these motors. The H-Bridge, shown in Figure 18, is a circuit that consists of four transistors

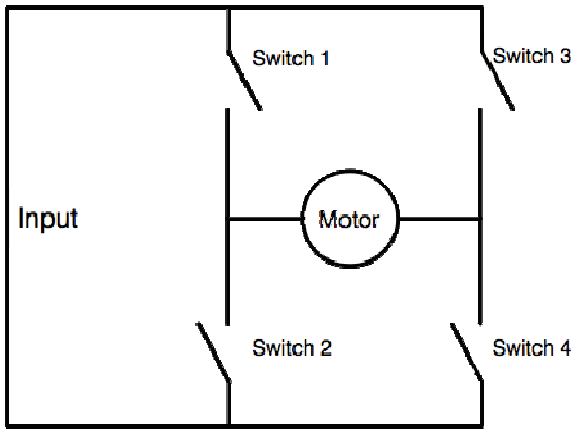

Figure 18 - H-Bridge Circuit

and a motor, along with the power source and a signal source. As shown in the diagram, there are two transistors between the positive power and the motor, and two more between the motor and ground. The motor is connected between opposite legs of the circuit, so that by turning diagonally opposed transistors, the motor will turn one direction, and by turning on the other pair it will turn the other direction. However, by turning off all the transistors, the motor is free to coast. By turning on both of the transistors that go to ground, the motor is locked.

Hydraulic and electrical circuits behave in extremely similar ways as well. Voltage and pressure are analogs, as are tubing and resistors, reservoirs and capacitors, and the

like. By converting this well established electrical circuit to its hydraulic analog, a valve system can be made that only required two inputs to switch between the four modes of operation. There are some changes in just how the system behaves though. In the electrical version, turning on all of the transistors would short out the voltage source, but turning on all of the valves in a hydraulic system is perfectly acceptable. Using the H-Bridge vastly simplifies the system, and allows for even more mechanisms to be run from a single CompactRIO. To the best of our knowledge, this type of hydraulic control system has not been developed before, so finding out if an H-Bridge could give us the desired fluid outputs was critical.

Encoder Design

The system needs to have an accurate feedback mechanism to ensure that any position errors are known by the controller. This could work either by finding a home position and keeping track of how far the system has traveled from it, or by keeping track of an absolute position. However, it would be far simpler for the system to pick up its operation after being manually positioned by the operator if it was using the absolute position method.

As no electronics can be used inside of the MRI, the encoder had to use fiber optics instead. The sensor would also need 12 bits to get the resolution needed with the travel that is also required. The array of 12 fibers would be arranged to read in the pattern printed on a sensor strip, which provides the exact location of the system output.

Preliminary Design

The first development stage of the project focused on developing a prototype proof-of-concept evaluation version of the mechanism without being concerned for clinical feasibility or MRI-Compatibility. Creating something almost entirely made from plastic with the machining capabilities on the WPI campus (primarily meant for metals) takes far more time and effort than using whatever material is convenient at the time. This design iteration would not be miniaturized either; its sole purpose is to test the basic concept of a pneumatic-hydraulic hybrid stepping actuator.

Pump

The prototype pump system, shown in Figure 19, consisted of a small syringe with the plunger attached to a double acting pneumatic cylinder. In this portion of the circuit, there is also a small hydraulic reservoir included to absorb the changes in system volume due to the single acting pump piston as well as any small leaks or flex in parts. The circuit also requires check valves to ensure that the pump will only send fluid forward into the valve system instead of back into the reservoir, and to make sure that fluid is drawn from the reservoir and not from the valves; this circuit is shown in Figure 20.

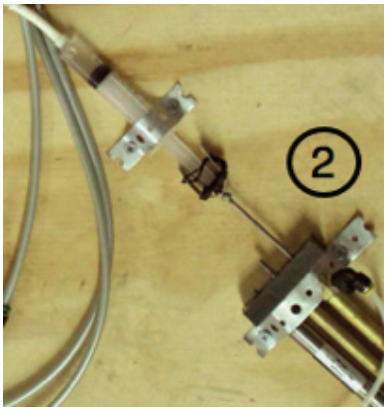

Figure 19 - Prototype Pump

Driven Piston

The driven piston was custom built, as manufactured hydraulic components are very expensive, and generally too large for even the prototype. Therefore, a custom cylinder was constructed using some steel tubing as the bore and a piece of aluminum with

two Buna-N O-rings as the piston. The challenge in making this was not these pieces though, but in sealing the ends of the cylinder while allowing fluid to flow in and out of both ends, and allowing the piston rod to exit the bore.

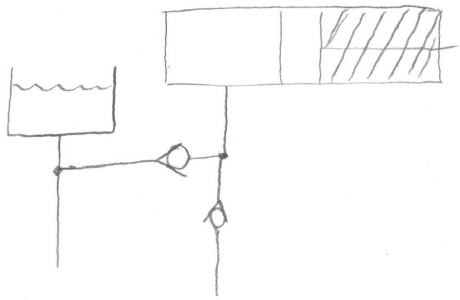

Figure 20 - Prototype Check Valves

To create the ends of the piston, PVC plumbing parts were used. One end was a single end cap with a brass hydraulic fitting screwed into a tapped hole put in using a lathe. The end cap was then attached to the steel as a loose press fit with a large amount of plumbing sealing adhesive. The end that needed to have a hydraulic input and a gland for the rod was trickier, however. For this we used a threaded end cap and a extender (male thread to female smooth). By putting the gland in the end cap and the hydraulic input coming out the side of the extender, this could handle both of the attachments without any leaks. The two parts were then screwed together and attached to the steel tube in the same fashion, this part can be seen at the top of Figure 21.

Valve System

To create the valve system, nonstandard valves would be needed to cut down the inputs to the ideal two, but by controlling readily available single valves in tandem, the same circuit can be emulated. This can either be accomplished by attaching each valve to a pneumatic solenoid and handling the pairing in software, or using a splitter on the pneumatic line to do so mechanically. With the parts available, solving the problem in software proved the simplest, so while all six inputs are used in the prototype, only four would be needed in an actual build; while only three would be needed if the pump piston

was switched to a single-acting cylinder. By using four pneumatically controlled hydraulic valves, the pump and driven pistons could be hooked up in a way that allowed for all four desired drive modes. In the prototype, two lines ran to the double-acting pump piston, and one to each of the valves in the H-bridge circuit. In the final build, the two lines for the pump can be reduced to one because of the spring-loaded single-acting pump system. The four valve control lines are operated in pairs, so in the next iteration, they will be reduced to two lines to decrease the number of channels.

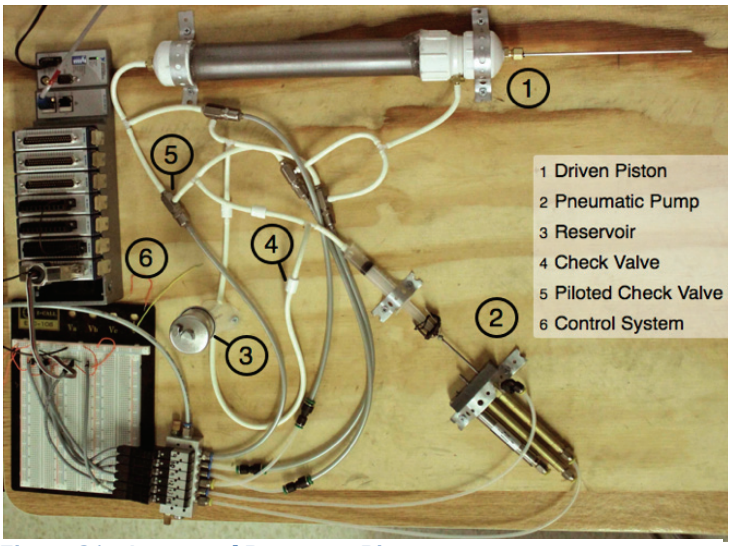

Figure 21 - Annotated Prototype Picture

These preliminary tests showed that the hydraulic H-bridge functioned exactly as intended by manually controlling the valves. Forward and reverse motions could be achieved very simply, and lock mode successfully prevented any motion in either the pump or the driven circuits. Coast mode was difficult to test, however, as the prototype driven piston had a lot of internal friction, even with the hydraulic fluid as a lubricant, so manual motion of this was slow and jerky at this design iteration.

Control System

To test the prototype further, the software could no longer be left out of the equation. The CompactRIO high power switch module was attached to the breadboard to handle the solenoids, and a LabVIEW program was developed to control the prototype. The knob controlled the drive mode, and pressing the step button handled a timed

sequence where the pump circuit pushed fluid out of the syringe, into the valve system, and then drew fluid back from the reservoir.

Adding the software revealed a problem with the prototype system. The fluid being used was mineral oil, due to its ready availability. Mineral oil has a very high viscosity, however, and in hydraulic systems fluid resistance is primarily determined by the viscosity of the fluid and the diameter of the passages it will be flowing through. Availability of parts on McMaster-Carr had kept the prototype tubing at 1/8th of an inch inner diameter, with this decreased even further while fluid flowed through the barbed connectors and valves. The high viscosity coupled with the small diameter components gave the system a very high fluid resistance. So while the prototype functioned as expected, the cycle time was very high. This would be easy to solve in a future iteration by enlarging the fluid passages and using a lower viscosity oil, however, and was not cause for undue alarm.

This prototype assembly, shown in Figure 21, proves that the hydraulic H-bridge circuit is capable of controlling the system in the way needed, and that careful control of the pump gives very accurate and high force motions on the driven piston. It also showed that the system can be automated with the only user input taking place on a computer screen. With the concept of the pneumatic-hydraulic hybrid actuator proven, the project moved into designing a version that was compact and MRI-compatible.

The encoder design was also tested at this stage in the development. A 12 fiber array of available fiber was created, and a few test sensor strips were prepared to help determine the best design for the future. These test rigs did not have a resolution anywhere near that of the final version, but they allowed for the concept to be tested in a less accurate setting.

Prototype Development

Mechanical

With the prototype working exactly as needed, the biggest challenge remaining was removing the steel that was used extensively throughout the construction, and shrinking the whole package down to something that would not crowd out the patient inside of the MRI. The subassemblies needed to build the system would not be readily available in any material other than metals, and the vast majority of these are steel. This means that unlike the prototype, essentially every part in the mechanism would need to be designed and built from scratch.

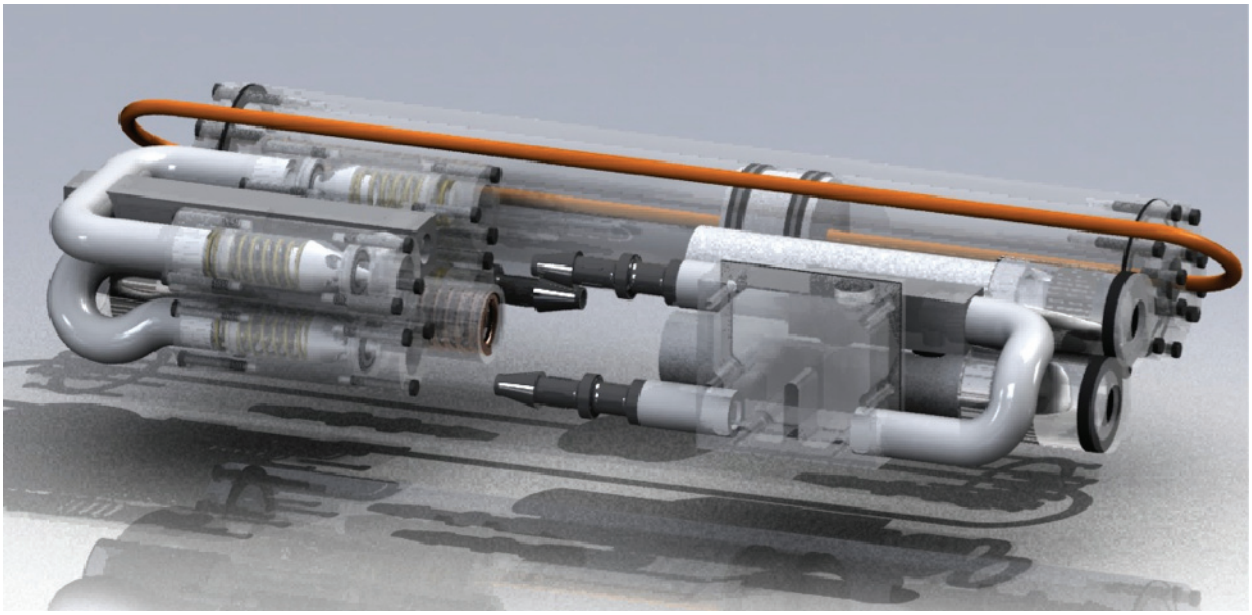

Figure 22 - Final Mechanism CAD

The entire mechanism, shown in Figure 22, was designed to be internally modular as well. This allows for each section of the assembly to be worked on individually, e.g. should the valve system have a problem, the valve block can be removed and worked on without disassembling the pump or the driven circuit. This also will allow for future versions of the actuator to be fit with alternate driven pistons or pumps to give more travel,

higher forces, or smaller or larger step sizes. This also allows for the design to be approached in sections instead of as an entire system. This simplifies each portion of the design, and sped up development time substantially, although it slightly increased the size of the finished product.

Pump

The first section in the mechanical system is the pump assembly, shown in Figure 23, and the first part of this to be acted upon in the pneumatic input. In the prototype assembly, a brass and steel cylinder was used, but this was much too large for what we needed to do, as well as being unusable inside of an MRI. Fortunately there were several samples of nonmetallic pneumatics to base a design off of. The usual construction method of these consists of a glass tube as the bore with a graphite piston cylinder.

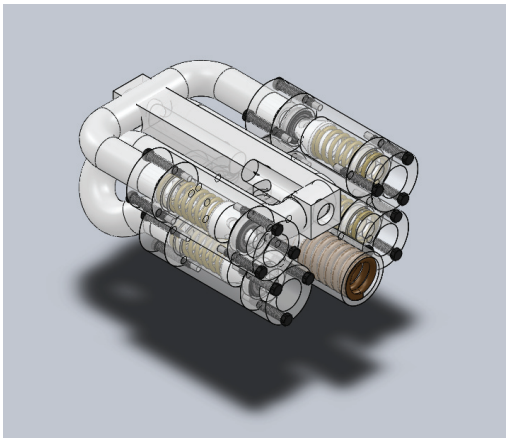

Figure 23 - Pump Assembly CAD

Another design change between the prototype and the final version was that the pump mechanism was to be changed to pump fluid as the piston moves in either direction, instead of only on one direction of the stroke. This eliminates the need for a large reservoir, as it no longer needs to absorb the volume changes of the pump, only those of the rest of the system as it flexes. It

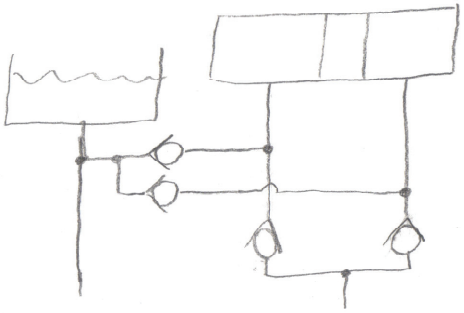

Figure 24 - Pump Check Valve Circuit

also allows for a much faster pumping time, as the piston is both pushing fluid out and drawing fluid in for the next cycle with the same motion. It is slightly more complex, however, and requires a more sophisticated check valve circuit around it, shown in Figure 24.

To continue down this route of compatible pneumatics, all of the pistons in the design would be made of graphite and use a glass bore. To reduce the machining required on the graphite pieces, which is challenging in the WPI shops, all of the assemblies with pneumatic inputs are designed to be single acting, so that the piston and the spring keep whatever is between them in place without fasteners in the graphite. This will be explained in more depth with each of these subassemblies.

With the pneumatic design principle determined, the pump design could continue. The next decision to make was what volume should be displaced with each pump cycle. However, to make this decision, we needed to know what the diameter of the driven piston should be. A brief look at the available plastic tubing sizes and the approximate desired size of the final assembly led to an assuming piston internal diameter of one inch, which meant that for the 0.004 inch displacement, which gave a pump volume of just over 0.003 cubic inches.

Figure 25 - Quad O-Ring

The diameter of the pump piston was then determined by the availability of quad style O-Rings, a cross-section of which is shown in Figure 25. These were critical for the pump to work as desired, as this ring geometry is designed for rapid oscillating motion. This led the design to a pump internal diameter of 0.210 inches, and a linear pump cycle displacement of just about 0.1 inches. The piston itself was made from brass, as it is too small and intricate to make

from plastic in the WPI shops. The tube that holds all of the pump components is made from polycarbonate for strength. The return spring is a bronze compression spring with a maximum load of 13.4 lb and a maximum displacement of 0.26 inches. This allows for plenty of range to adjust the step size.

The pneumatic input to the pump was constructed by sliding a glass tube over the main pump housing tube. This provides a piston diameter of 0.625 inches, which gives enough force to completely compress the bronze spring for the maximum step size. The graphite piston pushes against a garolite piston rod, used for its high rigidity despite a very small diameter, which is attached to the piston. The piston is connected to the spring via another garolite rod to a plastic disc used to press against the spring. The whole assembly, shown in Figure 26, is held captive by the pressure from the spring on one end and the air pressure on the other. This eliminates extra machining on the graphite, which is challenging, and keeps the piston piece itself relatively simple.

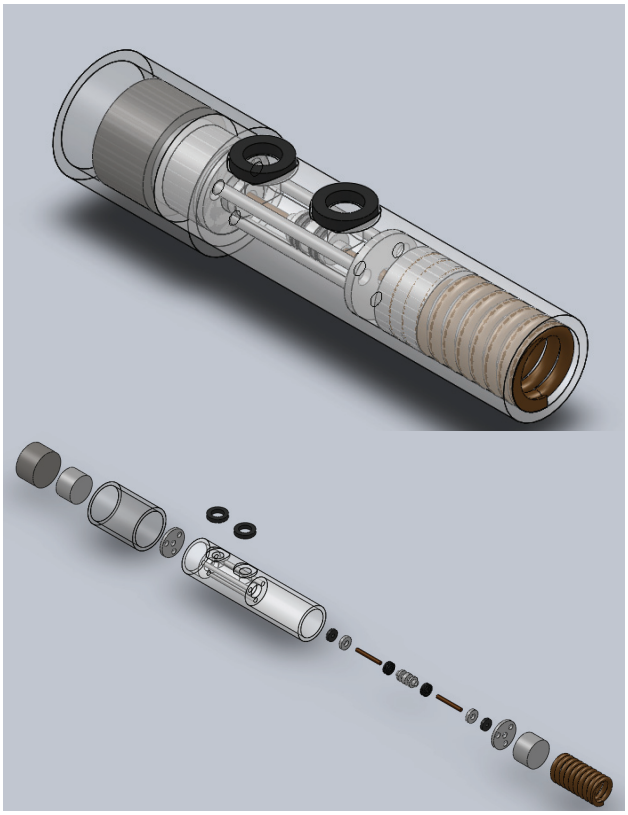

Figure 26 - Pump Tube Assembly

The pump circuit also requires check valves. These are used to turn the oscillations of the piston into well defined forward steps. Each end of the pump cylinder has a check valve between the reservoir and the pump, and another between the pump and the valves.

While the flow recombines after the check valves, all of these are needed to make sure that the pump does not recirculate any fluid while only forcing fluid forward through the system.

Hydraulic check valves are generally made from steel, and even in plastic construction check valves, the spring is still made from a ferrous material. This, along with the difficulty in finding small check valves with low fluid resistances, meant that they would need to be custom made. Check valves also come in two varieties: ball and dart. In a ball check valve, a sphere is kept pressed against a seal ring by a spring. When pressure is applied in the wrong direction, all it does is push the ball harder into the seal. However, when fluid pressure is applied in the other direction, it pushes against the spring, and opens the valve, allowing fluid to flow through. In a dart check valve, the ball is replaced with a cone. This geometry allows for the valve to operate at much higher frequencies, which definitely desirable in this application.

For the project to continue, custom MRI-compatible dart style check valves needed to be designed and constructed, the design and actualization of which are shown in Figure 27. The dart itself was made from PTFE for low friction against the polycarbonate casing. The spring was a brass compression spring from McMaster-Carr with a maximum load of about 4 pounds, and was preloaded slightly to ensure that small pressure oscillations would not open a valve in error. The seal ring is another quad O-Ring to allow the rubber to flex to accept any irregularities in the dart. Four of these, along with the pump tube itself, are arranged together to create the full pump circuit.

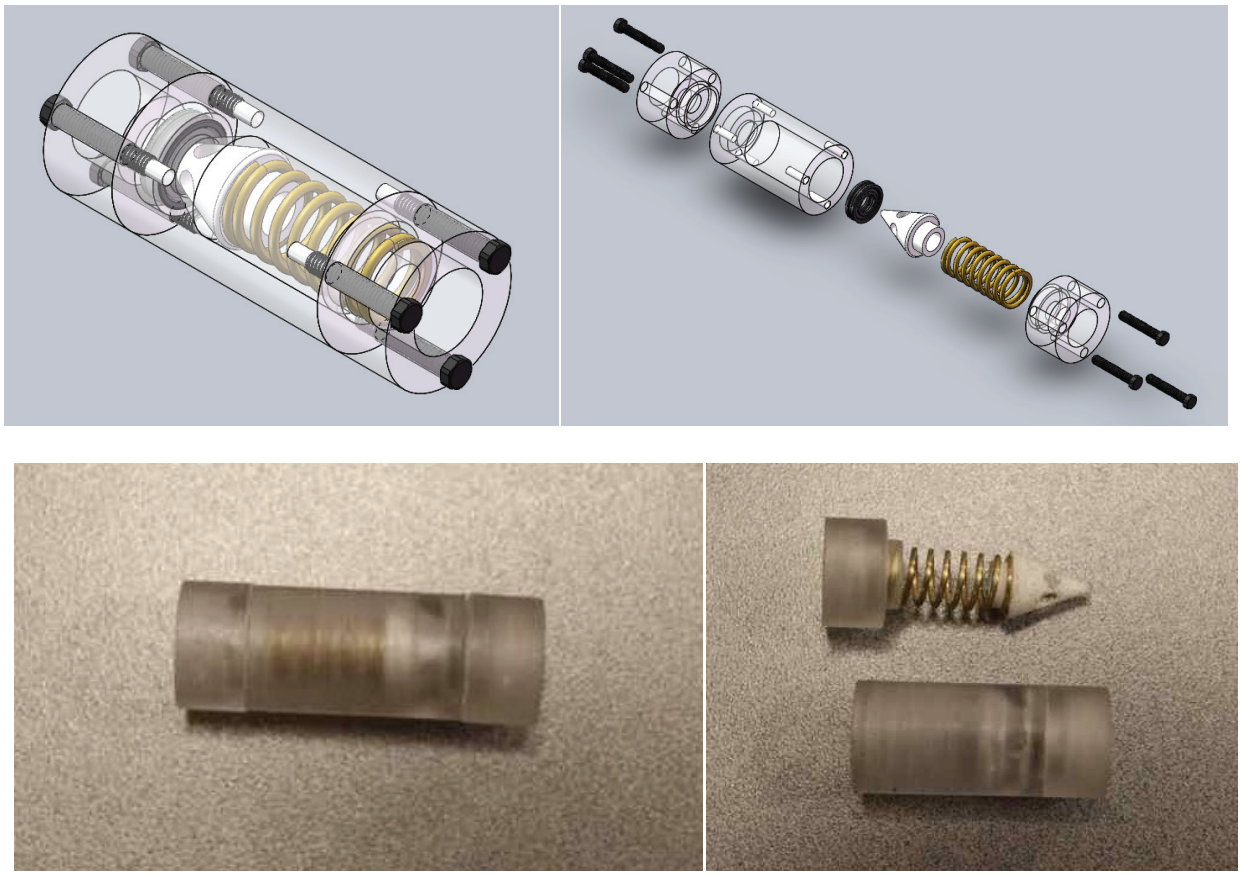

Figure 27 - Check Valve Design

Valves

The hydraulic H-Bridge circuit, shown in Figure 28, was easily the most challenging part of the mechanism to design. There needed to be four valves, controlled in pair, but in opposing corners of the circuit. This meant that to control the pairs of valves, shown in Figure 29, with a single pneumatic input, the manifolds would have to handle mapping the correct valves to the correct sides of the driven piston.

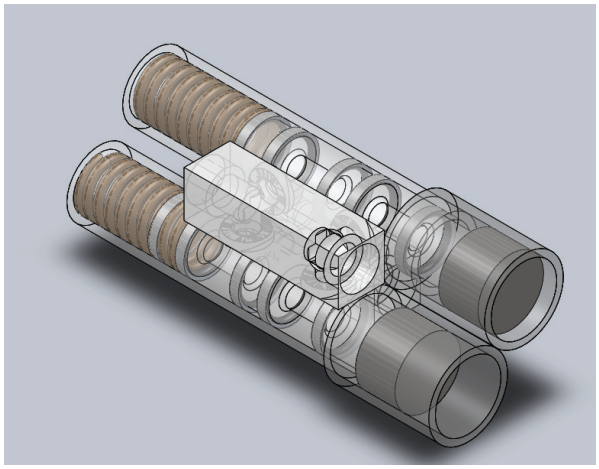

Figure 28 - H-Bridge

While the manifolds would require some tricky design work, the first step in designing this portion of the mechanism was to create a double valve with a pneumatic input and a spring return. To simplify the pneumatic design, the same design as the pump would be reused. This meant that the valve would once again be constructed from a tube. The tube would contain the return spring and the valve spool. The glass tube slides over the polycarbonate valve tube, and the graphite piston presses directly against the spool.

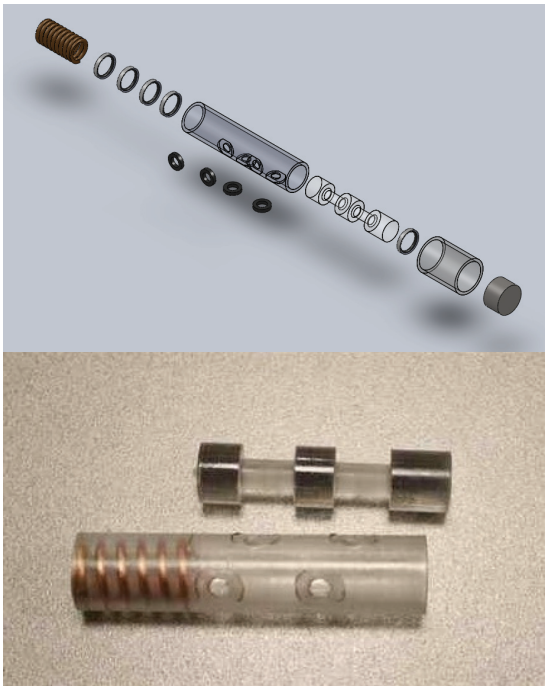

Figure 29 - Valve Design

The spool is the piece that determines what inputs are connected to which outputs. The tube has inputs on one side, and outputs ninety degrees opposed, with an offset between them. The offset allows for the spool to block the inputs when there is no air pressure applied to the pneumatic. When pressure is applied, the spool presses against the spring and shifts back to connect the inputs to the outputs, allowing flow through both channels.

The manifolds are the most intricate parts in the entire mechanism. The input manifold is simple, as the one input is connected to the nearest openings in the valves. The output manifold, shown in Figure 30, handles the crossover needed for the H-Bridge to function properly. The output on each side is connected to the nearest on one valve, but the far side of the other valve. This needs to be accomplished without restricting the flow of the fluid by reducing the passage diameter substantially, and without needing a large piece. The best way of doing this turned out to be making a manifold with an internal double helix. This met all of the requirements for the part, but is very difficult to make. The machining capabilities on campus made it impossible to cut from a block, but it could be made in the rapid prototyping machine without much trouble.

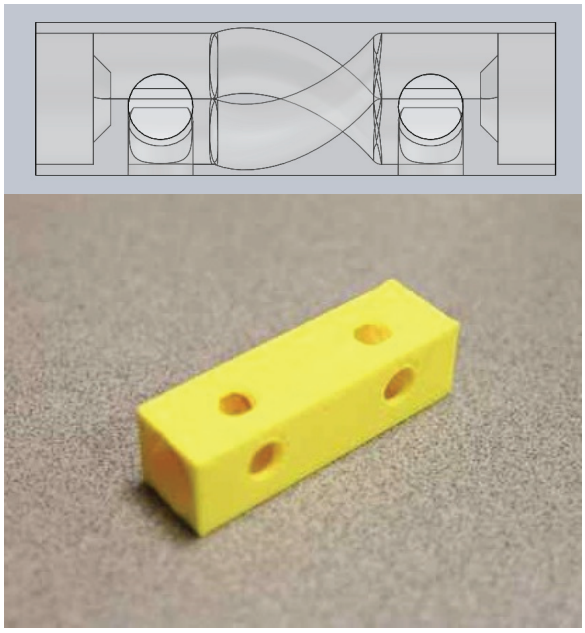

Figure 30 - Output Manifold

The fused deposition rapid modeling (FDM) prototyping machine (Stratysys Dimension) builds parts from ABS plastic by laying down lines of plastic. This,

unfortunately, leaves a porous surface in the finished piece. While is not ordinarily an issue for the parts the rapid prototype is used for, the hydraulic manifold could not have a porous construction, as fluid could move in unpredictable way. By creating a small test piece on the rapid prototyper, several different sealing methods were tested. Acetone was one possibility; it would dissolve the outer layer of plastic, and when flushed with water, would solidify into a solid skin. The acetone seeped too far into the plastic, and destroyed the structure of the part. Instead, by injecting the test piece with the plumbing adhesive used to build the prototype, and then removing the excess, the adhesive that seeped into the pores hardened and created a skin that fluid could not leak through. This allowed the printed part to be used as the output manifold of the valve system.

The valve block also contains the hydraulic reservoir for the mechanism. While the double acting pistons prevents large fluctuation in volume, a small reservoir is still important for ensuring that air can be removed from the system, and that any fluctuations caused by flex in the tubing could be absorbed without effecting the system function. The reservoir is also important for keeping the system supplied in the event of a small leak in the system and for trapping any air that may have entered the system. The reservoir is located at the equivalent of electrical ground; between the output of the H-Bridge and the input to the pump system.

Driven Piston

The driven piston is simply a large polycarbonate tube, with a plastic piston inside of it, using two more quad O-rings to seal the piston to the tube. The ends of the tube are sealed by bolting a plate down to the ends with a gasket between the plate and the tube end. These plates also have the openings for the hydraulic fluid to flow in and out.

The biggest challenge in the driven piston, shown in Figure 31, was keeping the output mechanism compact. First of all, the output piece needs to extend through both ends to keep the area, and therefore the step size, consistent. For a rigid rod to be used, it would need to extend out of the piston by the full travel on either end. This makes the assembly extremely large. By using a urethane cable instead of a rigid rod, the cable can go around pulleys after exiting the piston, and move a table on top of the mechanism and keep the whole mechanism compact. The biggest complication in using this is sealing the outputs, as the urethane will stretch more than a rigid material, and the stretch results in a matching reduction in diameter, as dictated by Poisson's ratio. Urethane, however, has a nonlinear Poisson's ratio, i.e. as more force is applied, the diameter decreases less quickly. By pretensioning the urethane cord, the forces applied by the actuator will not change the diameter of the cord enough to cause problems with the seals. This allows for a much more compact output method, and keeps the whole mechanism at a reasonable size.

Figure 31 - Driven Piston Design

Control System

For the control system of our design, we needed a device that would be capable of supporting both a graphical user interface as well as being able to support both analog and digital input and output devices. While not completely necessary, we were hoping that the final control system would allow us access to a field programmable gate array (FPGA) chip in order to interface with the encoders and possibly the pneumatic control logic as well. The advantage of that kind of setup would be that if the system was expanded to control multiple actuators, then it would be nice to read in all the encoder values simultaneously so as maintain a consistent state of the system. Even if only one actuator was used with the

control system, there was still the need to read in a 12-bit binary value, which would be most effectively done in parallel. The ability to have parallel operations occurring on the system allows for more consistent operation and should increase the safety and reliability of the system. There is also the advantage that processing through the FPGA, especially just combinational logic, can run exceptionally fast and not be potentially bogged down by other parts of the code vying for control of the CPU. In order to perform the requested functions, a small PC-104 computer system with an FPGA interface board was originally considered as that kind of setup had already been used in the lab for project work. Another option we had was using a CompactRio (cRIO) device from National Instruments (NI) as the team already had some experience with the system through its use in current *FIRST* robotics competitions. The cRIO also had all of the components that we required for our control system with the added benefit of having a chassis with interchangeable modules, so that we could configure it with exactly the inputs and outputs that we would need. We ended up working with NI to use one of their cRIO systems, as they are trying to get the device used in various kinds of projects to show its modularity and encourage its consideration during the design process. National Instruments ultimately donated a cRIO-9074 integrated chassis and controller system for our project, as well as 3 x NI 9403 TTL Digital I/O Modules, 1 x NI 9477 Sinking Digital Output Module, 2 x NI 9201 Analog Input Module, and 1 x NI 9263 Analog Output Module. This provided 96 DIO channels with the 9403 modules, allowing for six 12-bit gray code encoders and 32 sinking DO channels to operate the pneumatic valves for the actuators. The 9201 module could be used for pressure sensors or magnetic field sensors, as well as for the user interface, and the 9263s could be used for variable pressure valves.

Due to the need for extreme modularity in the final product, the National Instruments CompactRIO was an excellent fit for the control system. The I/O modules made it simple to maximize the number of actuators per controller, and the FPGA simplified reading the encoder and allows the system to be run more quickly and accurately, both of which are vital for the usability and safety of the mechanism.

Fiber Optic Daughterboard

The rest of the control system is implemented through the use of secondary daughterboard specifically for the fiber optics, the schematic of which is shown in Figure 32. The fiber daughterboard was constructed to act as an intermediary between the cRIO and the fiber optic cable. This was done to allow for signal conditioning outside of the scope of the cRIO analog input module. The inputs to the daughterboard were the 12 fiber optic strands that will carry the encoder information from the actuator assembly that can then be filtered through the microprocessor and output over 12 parallel TTL-level lines to digital inputs on the cRIO. The use of the digital lines on the cRIO allows for more encoders to be effectively used and provides a higher speed and more efficient interface than using the analog input directly. The filtering on the microprocessor was done because of the ease and dynamic reconfigurability of a digital signal processing

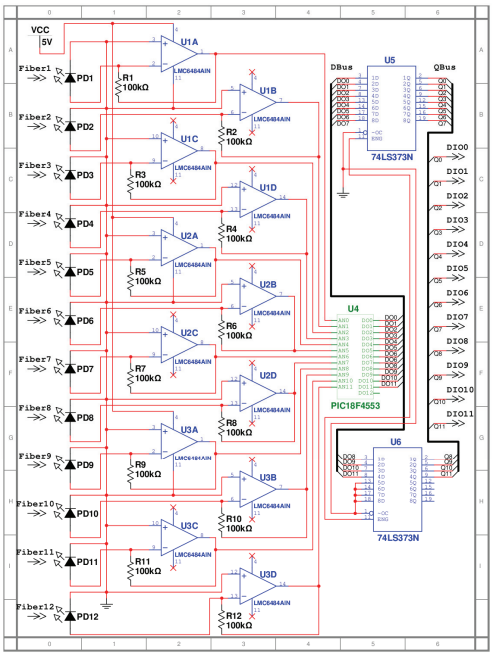

Figure 32 - Fiber Daughterboard

solution. This was accomplished by reading in analog voltage levels through analog-to-digital converters (ADCs) hopefully on the microcontroller itself. These voltage levels were derived from photodiodes, after conversion from a current output to a voltage and appropriate amplification.

This signal processing was facilitated on the fiber daughterboard by the use of a PIC18F4553 microcontroller from Microchip Technology Inc. This particular microcontroller was chosen primarily for its 13 on-chip 12-bits analog-to-digital converters (ADCs), in order to allow for the high level of precision that could then be achieved when thresholding the light intensities from the fiber optics, and its ability to be obtained in a PDIP form factor. In addition to these characteristics, this microcontroller also features a relatively high clock rate as well at RS-232 serial and USB support. While the USB support is not used for the current iteration of the daughterboard's design, that functionality might be a perk in the future. A dcPIC30F4013 would also work just as well for this application, but lacks USB support, and was ultimately not used based on the availability of multiple PIC18F4553 microcontrollers in case something went wrong.

Since the microcontroller can be dynamically reconfigured over a serial connection so that the thresholding levels can be set after the control system is initialized. In order to effect serial communication between the microcontroller and the cRIO, a MAX232 TTL to RS-232 level converter to convert between the TTL voltage levels from the PIC chip and the EIA-232 levels used for RS-232 serial communication. This is probably the most standard solution for this particular interfacing problem and thus has a fair amount of documentation and is why we chose it.

After the microcontroller was selected and its cRIO interfacing was established, the interface with the fiber optics themselves needed to be taken into account. In order to both transmit light to the encoder strip as well as to receive the intensity levels back, we needed to use matched IR LEDs and IR photodiodes. We decided to use SMA-905 to TO-18 adapters in order to interface the fiber optics to both the LEDs and photodiodes. This was done since there was cable available in the lab with SMA-905 connectors that we could use for testing, as well as the previous discovery that such adapters were commercially available. The fiber assembly is shown in Figure 33, along with the sensor read head. Given the specification of TO-18 packaging, we then needed to find LEDs that had as high of a radiant intensity as possible and photodiodes that had as high of a reverse light current as possible. We ultimately chose Osram SFH 483 GaAlAs 880nm LEDs because of their radiant intensity of 80mW/sr, which was one of the highest that was readily available in that packaging. Given the 880nm peak emission wavelength, we were able to find Vishay BPW24R 900nm photodiodes that were close enough, especially by looking at the response graph and finding that there was 0.96 relative spectral sensitivity at 880nm. These particular photodiodes were also selected due to their 60 μA reverse light current, one of the highest that we could readily find.

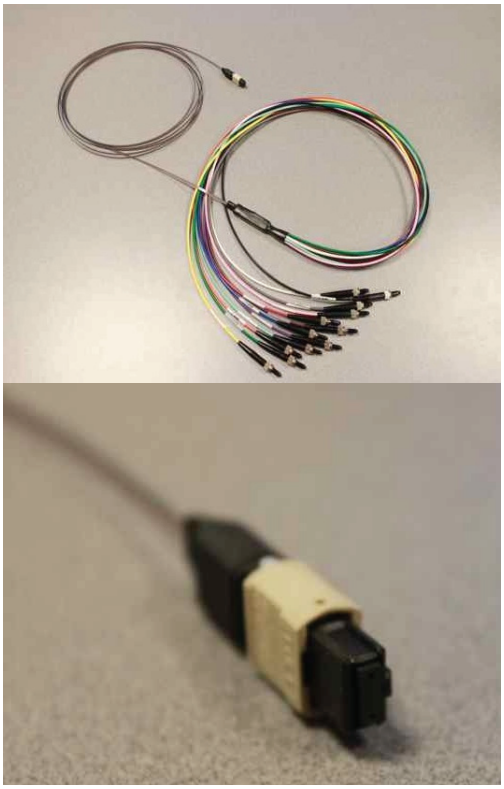

Figure 33 - Fiber Assembly

Since the photodiodes that we were using have a reverse dark current of 2 nA up to a reverse light current of 60 μA, we chose to feed this current output to an op-amp in a current to voltage configuration. Initially LM348 quad op-amps were chosen for use as the current to voltage converters, but it was quickly realized that the input bias current was too high to be effective when used with the photodiodes. For that reason, it was decided to use LMC6484 CMOS op-amps for that application. The difference being that the LM348 op-amps had an input bias current of 30 nA and the LMC6484 had an input bias current of 4 pA. The LM348 op-amps were still useful for additional amplification stages as were required due to the low level of light transmission through the fiber and thus a low level of radiant light intensity reaching the photodiodes. In order to provide a negative rail for the op-amps, an ADM8828ARTZ voltage inverter is being used. This voltage inverter uses a charge pump architecture to create the negative voltage and seems to be relatively standard for the given application.

Sensor Strip

The first challenge for the design of the linear optical encoder was the design of the encoder strip itself as defined by both the precision of the system as well as the size of the available fiber. Initially we tried to design the system to use fiber optic cable that we already had, at least for a first revision. Unfortunately what was available was too large for 0.1mm resolution, and thus two different aspects were analyzed at that point.

First, we looked to verify the operation of the fiber that we had available to us using a larger binary-reflected gray code strip just to visually test the light transmission through the fiber optic cable. This was sufficient to verify both operation of the cable, as well as the transmissive quality of that initial printed strip. Unfortunately, the initial print quality was less than desirable, exhibiting noticeable halftoning and it was determined that this would not be acceptable for the final iteration.

Second, we explored the possibility of altering the encoder strip itself so as to be able to use analog sensors and varying thresholding levels to determine position. This scheme was overly complicated and we were ultimately unable to create a pattern that met the design requirements without drastically increasing the number of individual fiber optic strands required. Because of these reasons, this approach was abandoned and focus was then directed on acquiring a fiber optic cable of the correct diameter and reverting to the original binary-reflected gray code. The disadvantage to using smaller fibers was that as

Figure 34 - Encoder Strip

the diameter decreases, the intensity of the light being transmitted decreases quadratically.

As we determined that a binary-reflected gray code encoder strip, shown in Figure 34, would work, further design work continued upon that premise. The reason why a binary-reflected gray code was used was first and foremost that that particular coding algorithm ensures that only a single bit of the code changes between each 0.1mm step, which is clearer in the magnified image in Figure 35. This is especially important so that a missed step can be accurately accounted for and the operator can be informed of such a fault condition with the system. Another key advantage to this kind of coding is that each position can be uniquely identified, meeting the absolute positioning design specification. This code can also be easily converted into the appropriate binary value for the step number using just only combinational logic with XOR, which is an advantage since that can easily be implemented on the FPGA of the cRIO and can thus run very quickly and accurately. Binary-reflected gray code is also an industry standard and frequently used in optical encoders, though usually in a rotary configuration.

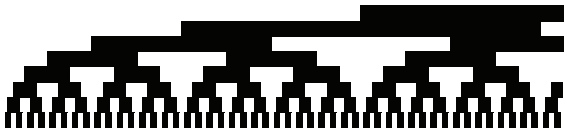

Figure 35 - Magnified Encoder Pattern

The encoder strip itself was ultimately printed with a laser printer on a transparency at 1200dpi as this was the best we could achieve using campus facilities. Much testing was done around campus to find the best print quality and then reviewed under a microscope to see how crisp it was. Ideally this process would probably be done professionally using a photolithography technique to achieve the highest level of accuracy as possible.

Programming

Just as with the control system itself, the programming was split up into two different parts. Some code resides on the cRIO itself and some resides on the PIC microcontroller located on the fiber daughterboard. Since each part of the control system is intended to provide different functionality, the code for each part is specifically written with its intended purpose in mind.

The programming for the cRIO is itself split into two parts as the chassis includes both a PowerPC central processing unit (CPU) and an FPGA chip. The advantage of those two separate pieces of hardware was that the processor is capable of running both sequential and interrupt-driven code as well as performing arithmetic operations while the FPGA can provide nearly real-time processing of digital logic. For these reasons, it made sense to have the front panel code running on the CPU and the sensor interfacing and pneumatic control logic code use the FPGA for processing. In order to effect this operation, the cRIO was programmed using National Instruments LabVIEW with the Real-time and FPGA modules.

The basic premise used for structuring the LabVIEW VI, shown in Figure 36, was that the appropriate VIs needed to reside on the appropriate targets and that everything needed to be as modular as

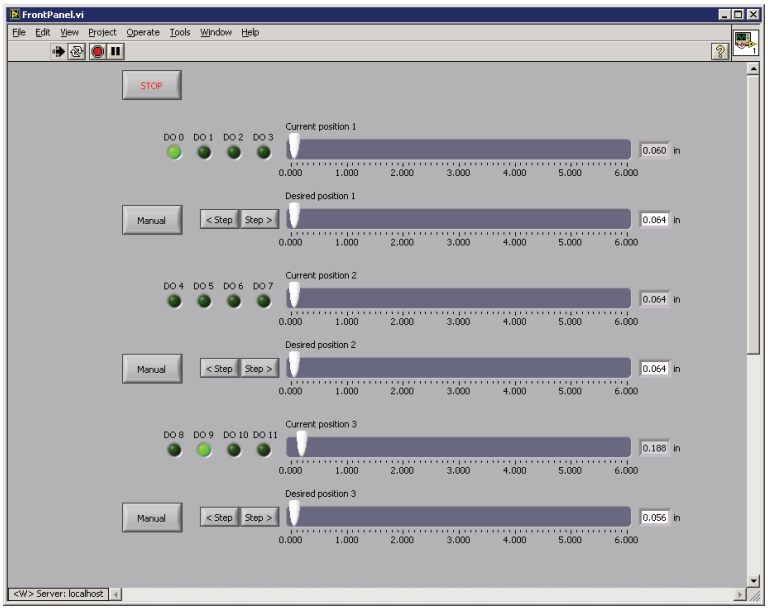

Figure 36 - Actuator VI

possible. A sub-VI was written for the FPGA to handle the conversion from gray code to a binary position value and was easily effected using just XOR gates in combinational logic. A sub-VI was also written that takes input about the current position of the system and the desired position of the system and calculates the output values for the valve control to set the appropriate direction on the H-bridge as well as to determine whether the pneumatic pump should be pumping or not. The front panel was ultimately constructed to be run on the CPU of the cRIO and interfaces with the appropriate sub-VIs to control the system. The reason to use sub-VIs was that they work similarly to subroutines in other programming languages and allowed the control system to be expanded to control up to 6 actuators under the current state of the system.

For the PIC microcontroller, there were only really two options for how to program it, C and assembly. Ultimately most of the code is written in C with a few sections written in assembly. C was used since it is much easier to code with and could be used to implement all the functionality that was asked of it. The small bits of assembly code were used mostly for low-level operations like manipulating on-chip memory. All of the code for the PIC microcontroller was compiled with the PIC18 C and ASM compilers and is relatively simple. The main function just sits in an infinite loop like most embedded systems stepping through the ADC channels and reading in each of their values. These values are then thresholded to the configured levels and outputted to a set of flip-flops in order to latch the current step value to be read by the cRIO.

Validation

Encoder

At the end of this project, the concept of the linear absolute optical encoder has been proven. There has been no good way to accurately position the read head at this point, as the mechanical assembly has not progressed to the level where this sort of alignment accuracy can be achieved. However, the initial prototype fiber cable has been used to test a large scale, low resolution encoder strip, and the concept has been shown to work.

The fiber daughterboard has been prototyped and tested outside of the fiber optic sensor. By directly illuminating the photodiodes, use of the full range on the PIC ADC is observable. Background lighting provides a readable signal, and covering the photodiodes brings the reading very close to zero. This means that the photodiodes, the current to voltage conversion circuit, and the PIC ADC are all working. The thresholding has been programmed, but is not currently implemented. This is because the current fiber setup does not provide enough light to give a reliable reading on the PIC ADC. By adding additional amplification to the daughterboard circuit, this problem can be resolved, and all that still needs to be set in the PIC are the thresholding cutoff values. The code is ready for these to be configurable over a serial connection, however the hardware for this has not yet been implemented.

Mechanical Design

The mechanical portion of the system is still largely in the manufacturing stage. The subassemblies (e.g. pump tube, check valves, valve tubes, etc.) are completed, however the housings for the system that keep everything together have not yet been finished. These are large rapid prototyped components, and the lengthy lead time and tricky design of

these components has delayed their completion. The components have been tested in isolation from the rest of the system, and function as they were intended. The system is able to function without housings, but this plan has not been implemented yet.

The design itself should fulfill all of the design requirements, the travel is exactly the six inch requirement, and the desired step size of 0.1mm is well within the tunable step size of up to 0.25 mm. The valve system locks at a pressure loss and prevents any uncontrolled motion. The hydraulic H-bridge gives the mechanism all of the desired modes with only two pneumatic inputs, and the whole package fits within a 1.5 by 5 by 9 inch box. The only metal pieces in the entire mechanism are the brass and bronze springs, and the brass pump piston, and all electronics have been removed from the actuator assembly.

Programming

The LabVIEW code has been finished, but not fully tested, once again because of the mechanical assembly status. The gray code encoder decoder has been proven to work, and can handle the resolution and time constraints imposed on it. The control loop for the system also works, and determines the correct H-bridge configuration and pump cycle based off of the desired location and the actual location of the driven piston. The GUI is set up to handle up to six actuators, but can easily be scaled back for any multi-actuator application that this mechanism was designed for.

System Integration

The system is, at the moment, still not fully integrated. The systems have all been tested separately, and the software and mechanical portions have been tested together on the prototype, however the current status of the mechanical assembly has prevented full system integration and testing. There are no foreseeable issues with this, as all components have been tested with simulated inputs from the other portions of the actuator.

Discussion

This project successfully developed a pneumatically-controlled, MRI-compatible linear stepping actuator with real-time position feedback. The design fulfilled the requirements for precision, travel length, and force output. The hydraulic H-bridge circuit is a novel approach to a complex control problem, and is capable of providing the four drive modes from only two inputs. The modularity requirement has been used as basis for nearly all of the construction choices. Each portion of the hydraulic system was designed as a separate module so that they can be swapped out to provide different step sizes, travels, and/or forces. The actuators have also been designed to have the upper portion of the case move; this allows for the actuators to be stacked on top of each other to provide multiple axes of motion.

The quantitative design goals for the project have all been met. The 6 inches of travel requirement defined the current version of the driven piston as well as the length of the sensor strip. These components are designed to be easily changed to allow for any travel needed. The step size is adjustable, but 0.1 mm is in the middle of the current adjustable range, and the force requirement has been far surpassed, with a maximum output of 300 pound-force. This assumes that the force of a fully compressed spring is applied to the fluid; in general operation the actuator will provide a force more on the order of 30 pounds, still far more than was required. The end-to-end travel time has yet to be tested, unfortunately, as the assembly must be completed for this. The 15 second target is quite feasible as the fluid passages are all extremely large for the fluid flow velocities in question.

Future Works

The mechanical portion of the project still needs to have a couple of pieces still finished. The input manifold still needs some minor machining, as does the pump manifold and the driven piston end caps. All machining should be completed within a week of this report being turned in. The larger mechanical problems remaining are to finalize and test fit the housings and assemble the mechanism in a realistic fashion. Testing outside of the housings should prove that the basic concept of this design iteration is successful; without the actual housings, the system will not behave as it would in its final setup. The actuator has also not been tested inside of an actual MRI machine. The system has been built to the highest standards of MRI-compliance, however, and this should not be a problem.

The electrical and control systems, while functional independently of each other, need to be integrated together. A large step toward this integration would be the transition of the fiber daughterboard to a printed circuit board (PCB) so that the components that do not interface well with a breadboard can be incorporated into the system. The integration would also allow for the serial configuration subsystem to be utilized. In addition to the electrical and control systems being integrated together, the encoder strip needs to be mounted to the mechanical portion of the design. This includes mounting of the fiber optic read head as well as a fiber to transmit the backlight to the encoder strip, potentially with some sort of light guide to spread out the backlight across all 12 fibers on the read head. To interface the fiber with the electrical system, the SMA-905 to TO-18 adapters need to be mounted and the IR LED needs to be pulsed to maximize its radiant intensity.

Once these tasks have been completed, the first actuator will be ready for testing. At this stage, the accuracy of the assembly will need to be verified, and the pump will need to

be tuned to give the proper step size. There is also the chance that one or more of the subassemblies will need to be modified. None of the components have been tested in a full assembly, so there could still be some issues getting them to work in concert.

After accuracy testing and MRI-compliance testing, the actuator needs to be replicated to test their modularity and attempt to make a multi-axis assembly. This will allow for the control software to be integrated with the output of the MRI to allow the system to be controlled by the surgeon based on the patient's status. Once this is ready, the system needs to be tested in its final, clinical setting. Once this capability has been established, the actuator will be completed and tested, and is ready for widespread use in MRI robotics.

Works Cited

1. Liang, Zhi-Pei, and Paul C. Lauterbur. Principles of Magnetic Resonance Imaging: a Signal Processing Perspective. Bellingham, Wash.: SPIE Optical Engineering, 2000. Print.

2. Kuperman, Vadim. Magnetic Resonance Imaging: Physical Principles and Applications. San Diego: Academic, 2000. Print.

3. Lux, Matthew M., et al. "Ergonomic evaluation and guidelines for use of the daVinci Robot System." *Journal of Endourology* 24.3 (2010): 371+. *Academic OneFile*. Web. 28 Apr. 2010.

4. "The Basics of NMR." *RIT CIS - Center for Imaging Science*. Web. 18 Nov. 2009. <http://www.cis.rit.edu/htbooks/nmr/inside.htm>.

6. Young, Stuart W., and Stuart W. Young. Magnetic Resonance Imaging: Basic Principles. New York: Raven, 1988. Print.

8. De, Wolf David A. Essentials of Electromagnetics for Engineering. Cambridge: Cambridge UP, 2001. Print.

9. Gilbert, John, Greg Wheeler, Richard Lingreen, and Robert Johnson. "Skip Navigation LinksHome April 2006 - Volume 19 - Issue 2 Open Stand-Up MRI: A New Instrument for Positional Neuroimaging" *Journal of Spinal Disorders & Techniques* 19.2 (2006): 151-54. Web. 2 Jan. 2010.

10. Tabelow, Karsten, et al. "High-resolution fMRI: Overcoming the signal-to-noise problem." *Journal of Neuroscience Methods* 178.2 (2009): 357+. *Academic OneFile*. Web. 27 Apr. 2010.

11. "Implantable linear motor is made of piezoceramics for MRI." *Advanced Materials & Processes* 163.7 (2005): 55. *Academic OneFile*. Web. 27 Apr. 2010.

12. Hashizume, Makoto. "MRI-guided laparoscopic and robotic surgery for malignancies." *International Journal of Clinical Oncology* 12.2 (2007): 94+. *AcademicOneFile*. Web. 27 Apr. 2010.

13. Muntener, Michael, Alexandru Patriciu, Doru Petrisor, Dumitru Mazilu, Herman Bagga, Louis Kavoussi, Kevin Cleary, and Dan Stoianovici. "Magnetic

Resonance Imaging Compatible Robotic System for Fully Automated Brachytherapy Seed Placement." *Urology* (2006): 1313-317. *2006-muntener-urology.pdf*. Elsevier. Web. 27 Apr. 2010. <http://urobotics.urology.jhu.edu/pub/2006-muntener-urology.pdf>.

14. Weston, Richard, and Junsheng Pu. "Motion control of pneumatic drives." *Microprocessors and Microsystems* 12.7 (1988): 373+. *Academic OneFile*. Web. 28 Apr. 2010.

15. Fischer, Greg, Axel Krieger, Iulian Iordachita, Csaba Csoma, Louis Whitcomb, and Gabor Fichtinger. "MRI Compatibility of Robot Actuation Techniques – A Comparative Study." *MICCAI 2008*. Web.

16. Y. Yu, T. Podder, Y. Zhang, W. S. Ng, V. Misic, J. Sherman, L. Fu, D. Fuller, E. Messing, D. Rubens, J. Strang, and R. Brasacchio, "Robot-assisted prostate brachytherapy," Medical Image Computing and Computer-Assisted Intervention - MICCAI 2006. 9th International Conference. Proceedings, Part I (Lecture Notes in Computer Science Vol. 4190), (Berlin, Germany), pp. 41–9, Springer-Verlag, 2006.

17. K Chinzei et al. (2000), Surgical assist robot for the active navigation in the intraoperative MRI: Hardware design issues. Proc IEEE/RSJ Int Conf on Robotics and Intelligent Systems (IROS): 727-32

18. Elhawary H, Zivanovic A, Rea M, Davies B, Besant C, McRobbie D, Lamperth M, "A Modular Approach to MRI Compatible Robotics: Interconnectable One DOF stages," IEEE Engineering in Medicine and Biology Magazine, Special Issue on MR Compatible Robotics, accepted for publication.

19. "World's first nonmagnetic robot arm." *Machine Design* 80.8 (2008): 40+. *Academic OneFile*. Web. 29 Apr. 2010.

20. Melzer, A.; Gutmann, B.; Remmele, T.; Wolf, R.; Lukoscheck, A.; Bock, M.; Bardenheuer, H.; Fischer, H.; , "INNOMOTION for Percutaneous Image-Guided Interventions," *Engineering in Medicine and Biology Magazine, IEEE* , vol.27, no.3, pp.66-73, May-June 2008

21. Zu-yan, MEI "Mechanical Design and Manufacturing of Hydraulic Machinery," Aldershot, Hants, England: Avebury Technical, 1991. Print.

22. Miller, John E. "The Reciprocating Pump, " Malabar, Florida: Kreiger Publishing Company, 1995. Print.

23. Pippenger, John J; Hicks, Tyler G. "Industrial Hydraulics," New York: Mc-Graw Hill Publishing, 1979. Print.

Appendices

CAD Models

All prepared renders are in this appendix, the full CAD models can be found in Solidworks format on a CD attached to the report or on file with Prof. Fischer.

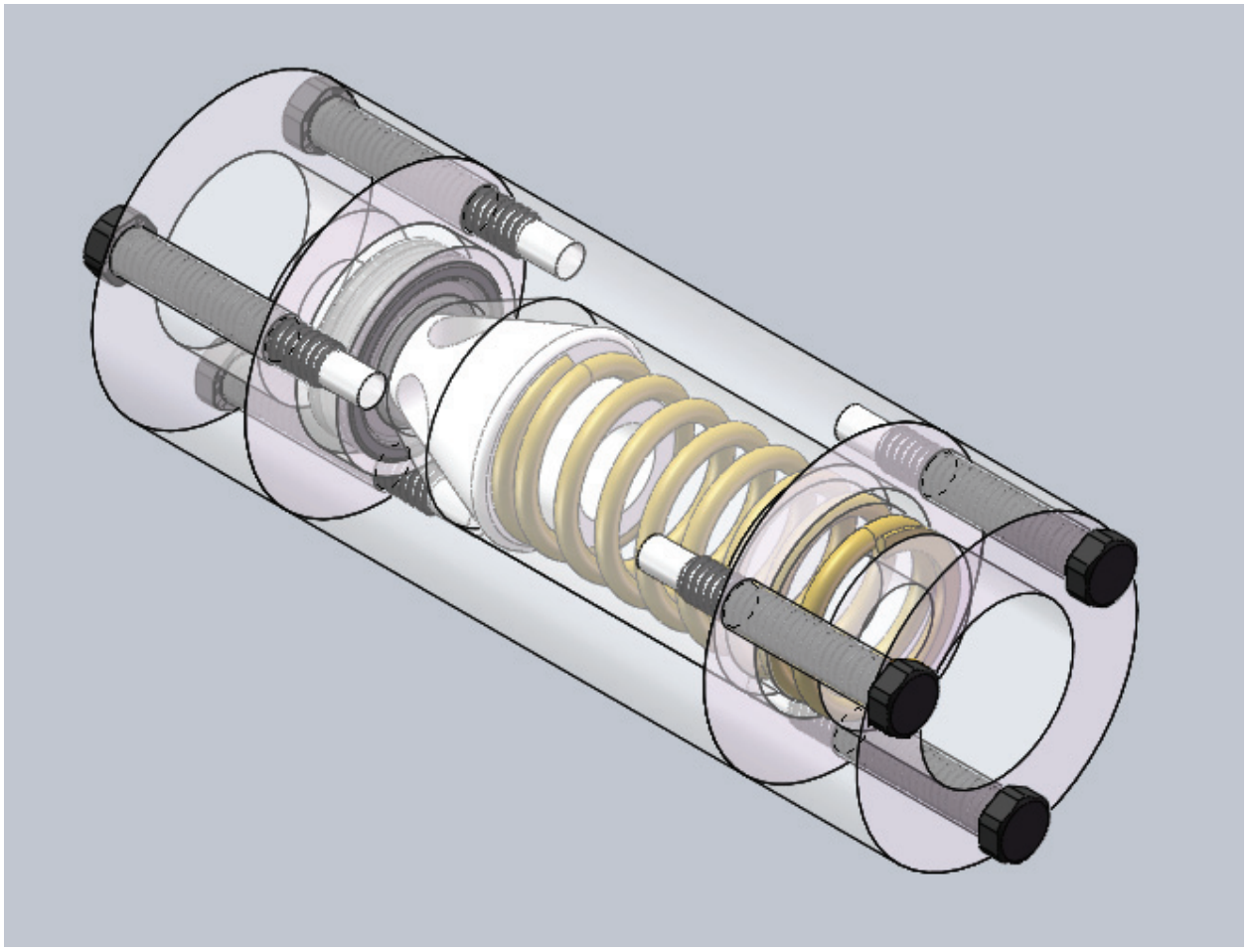

Check Valve

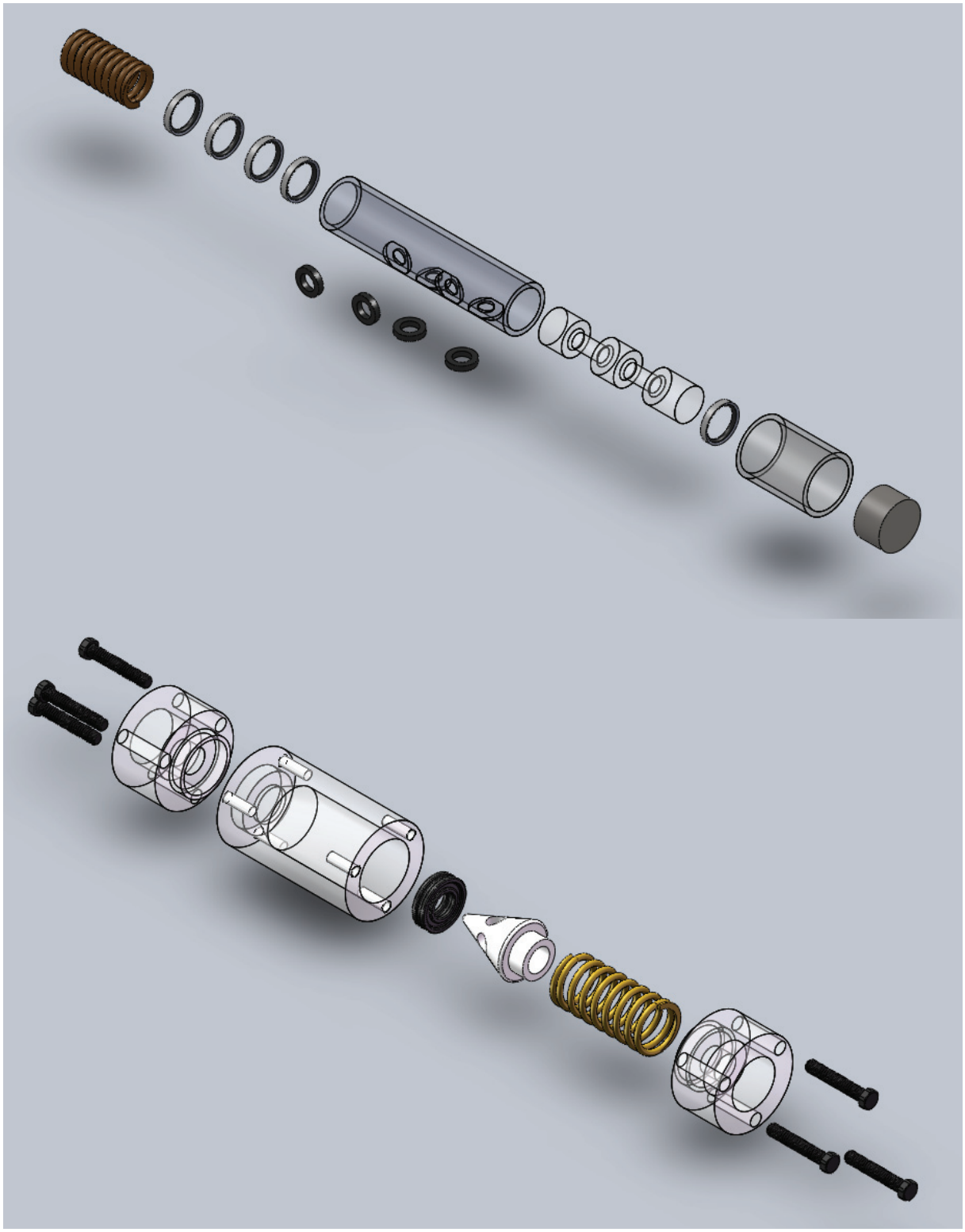

Check Valve (Exploded View)

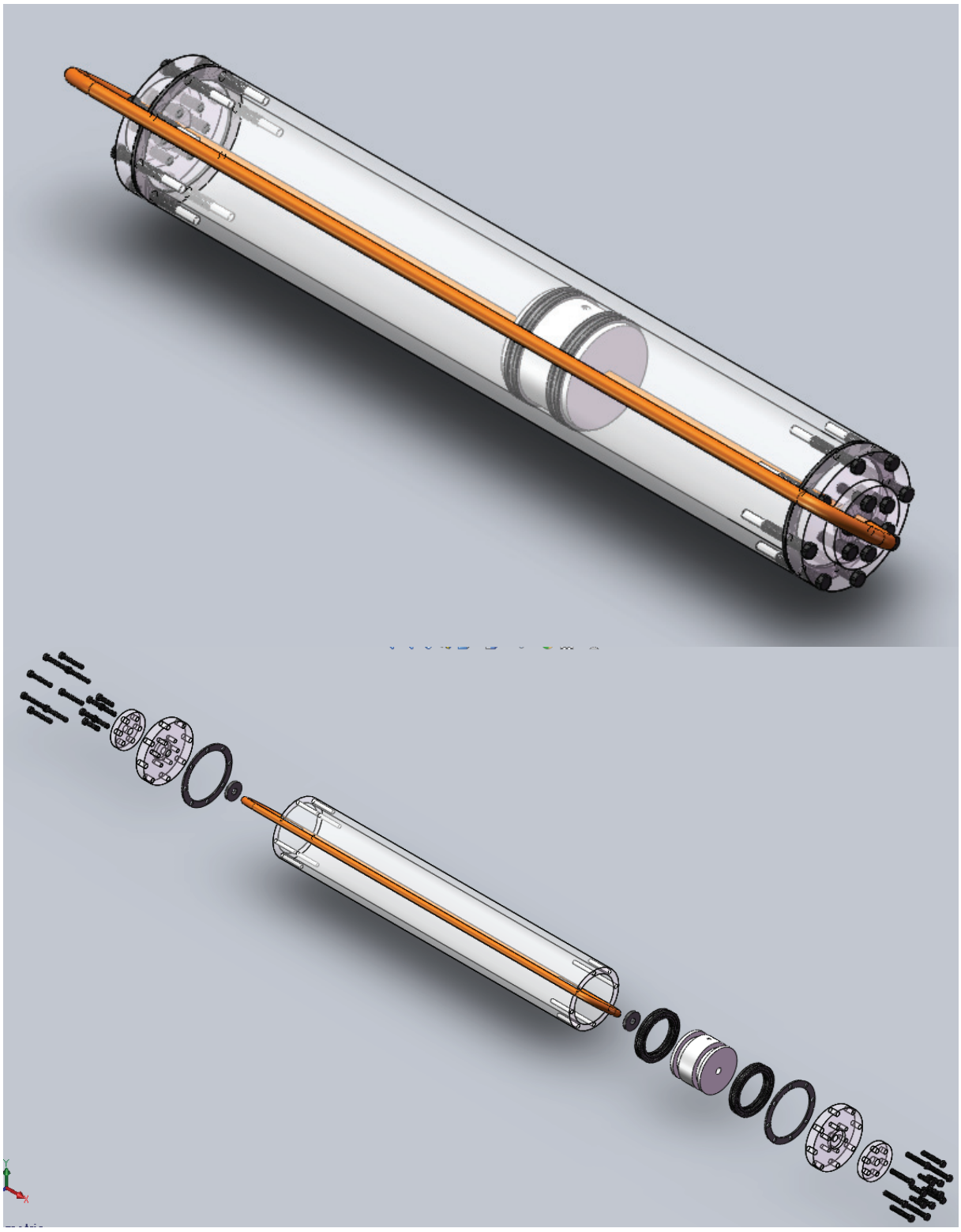

Driven Piston

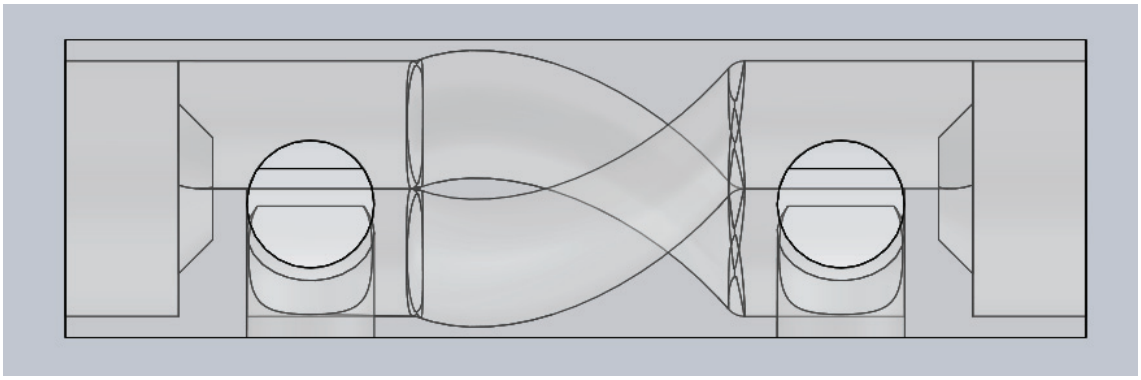

Manifold

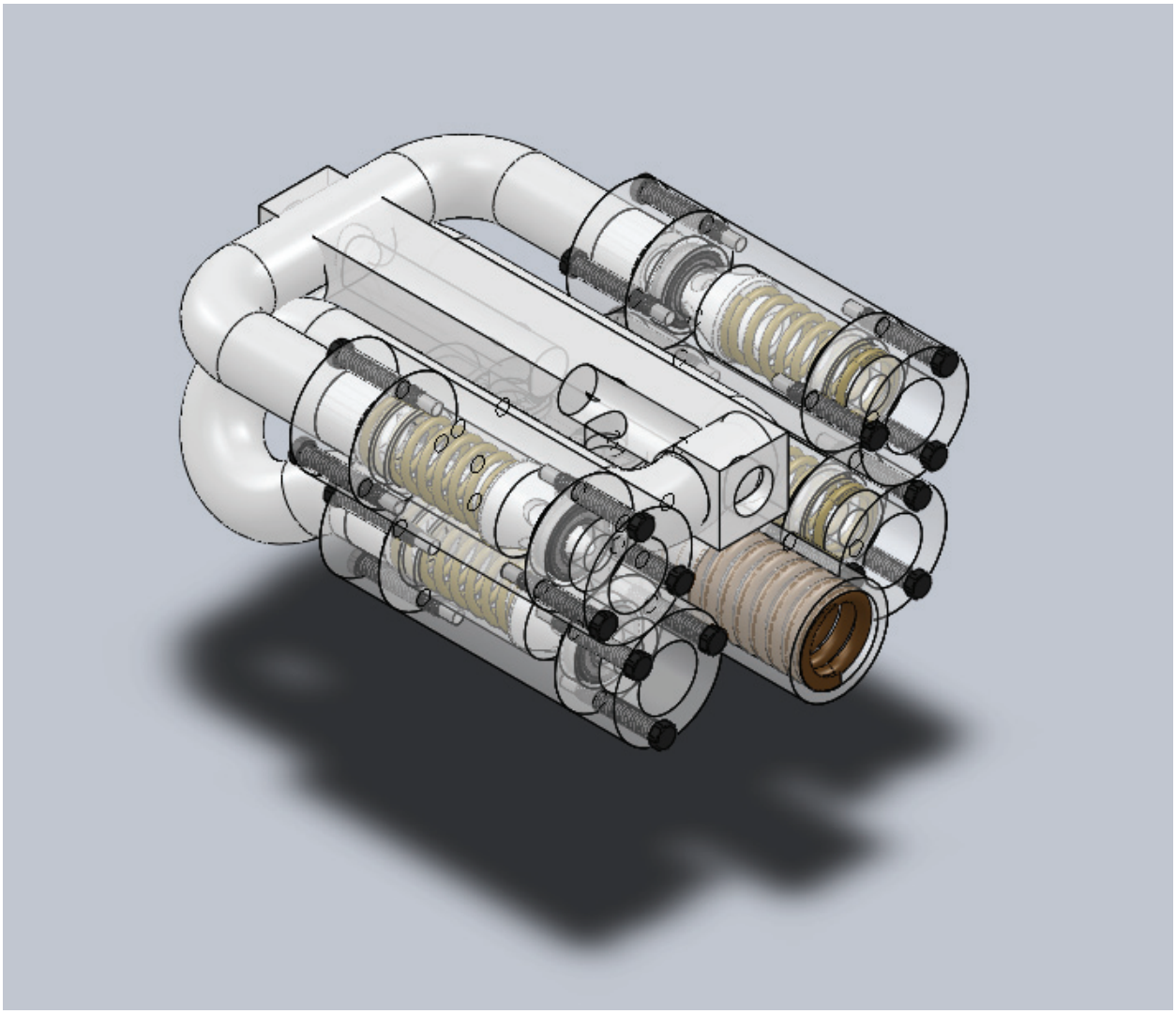

Pump Assembly

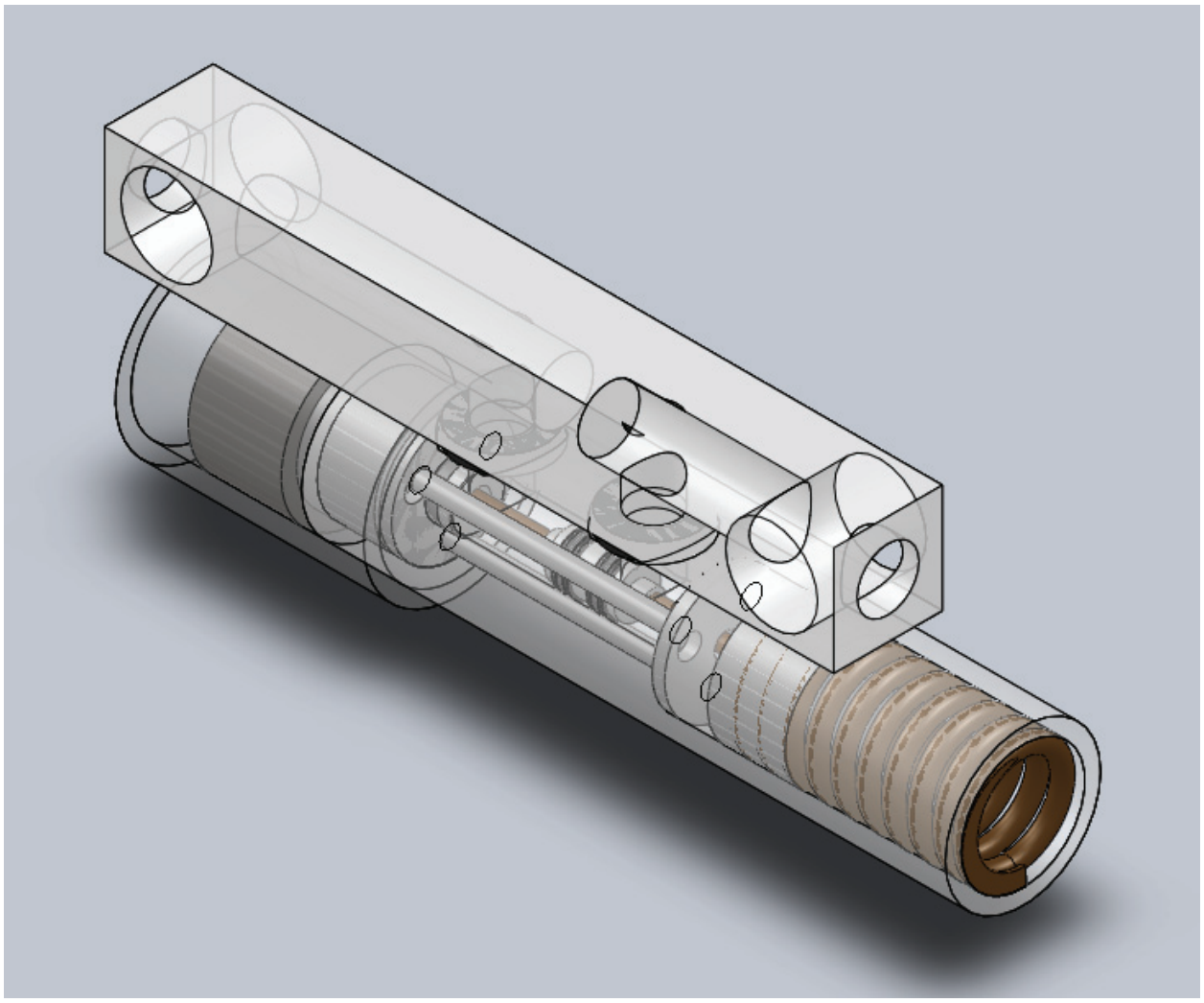

Pump and Manifold

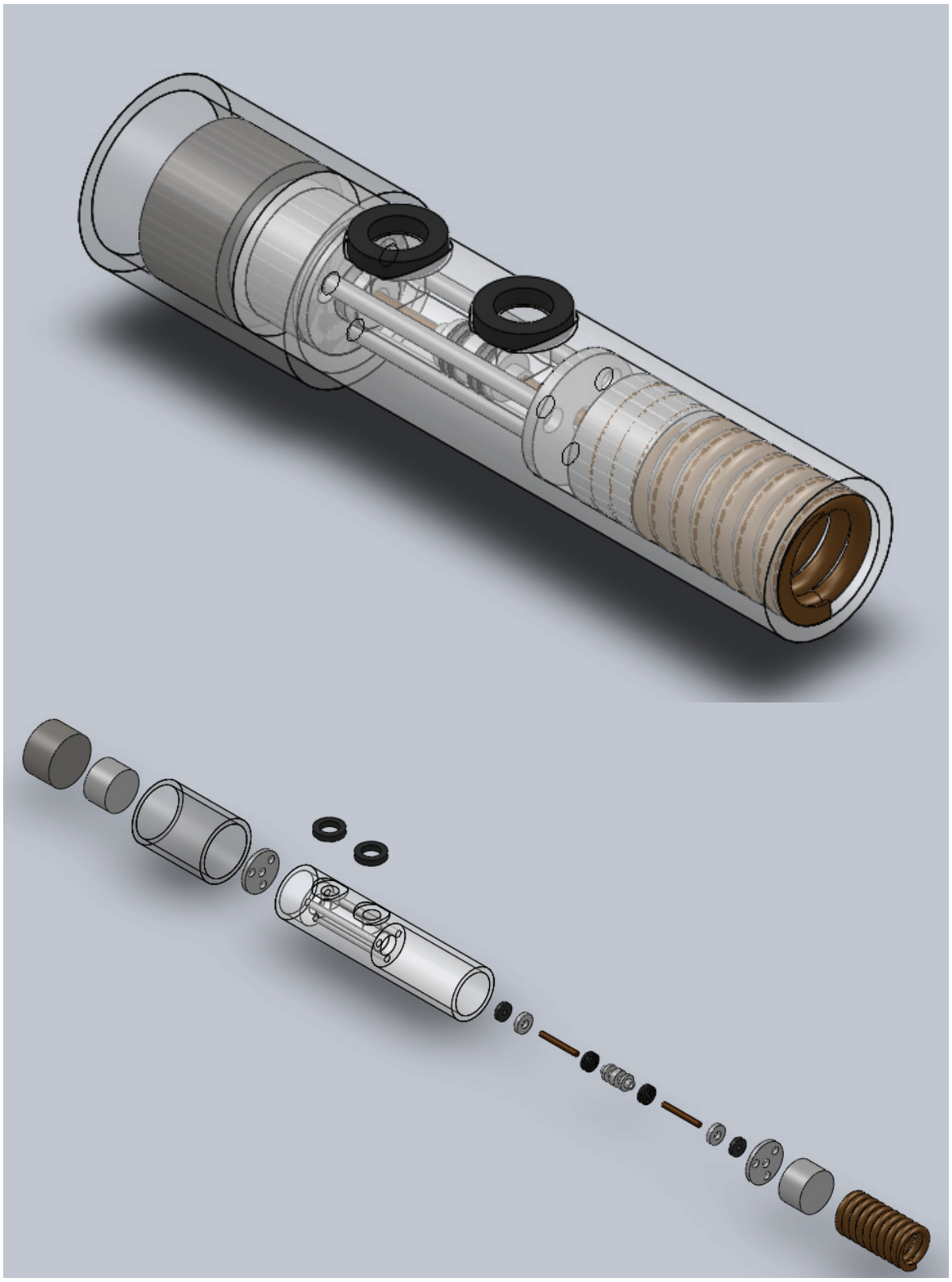

Hydraulic Pump

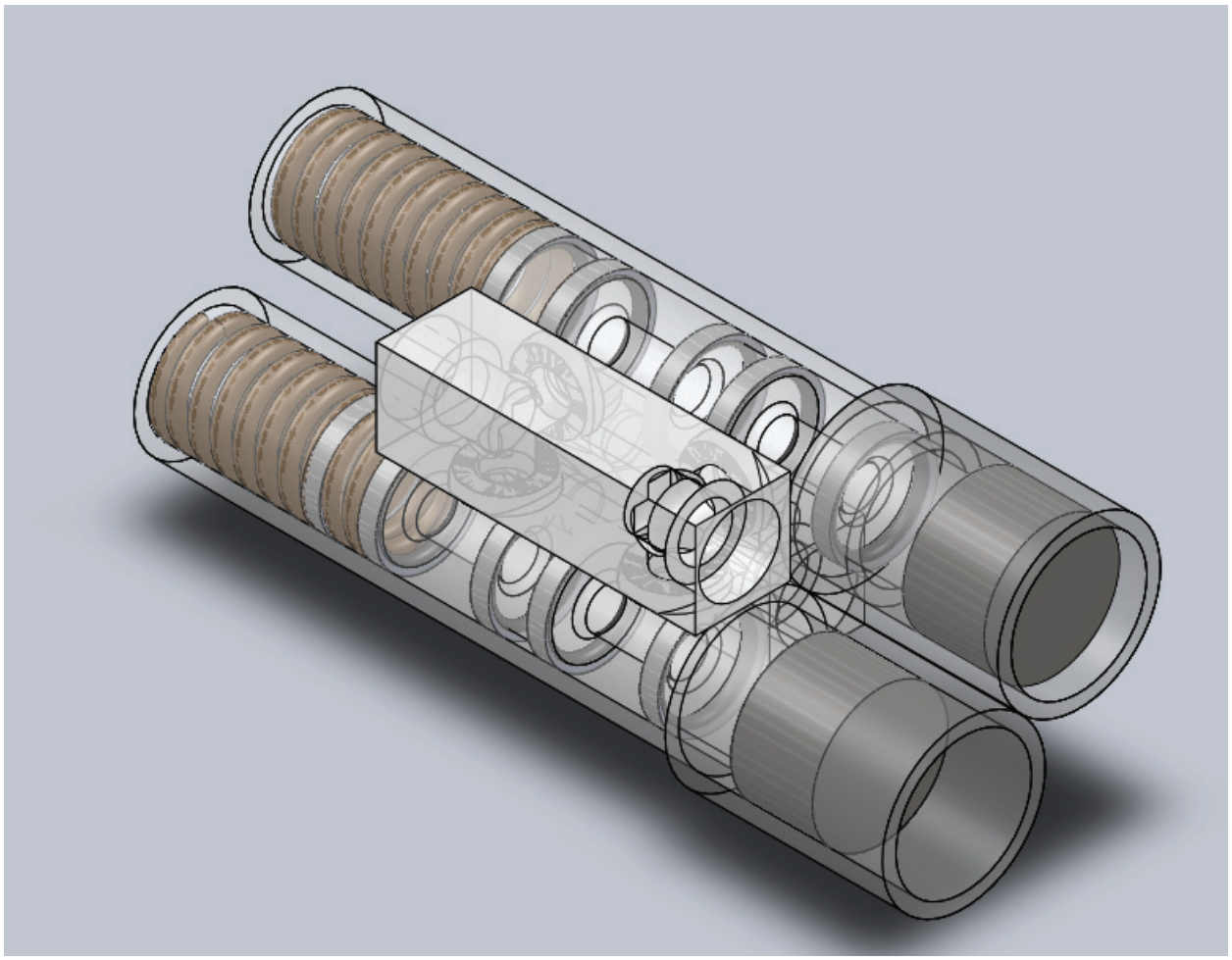

H-Bridge

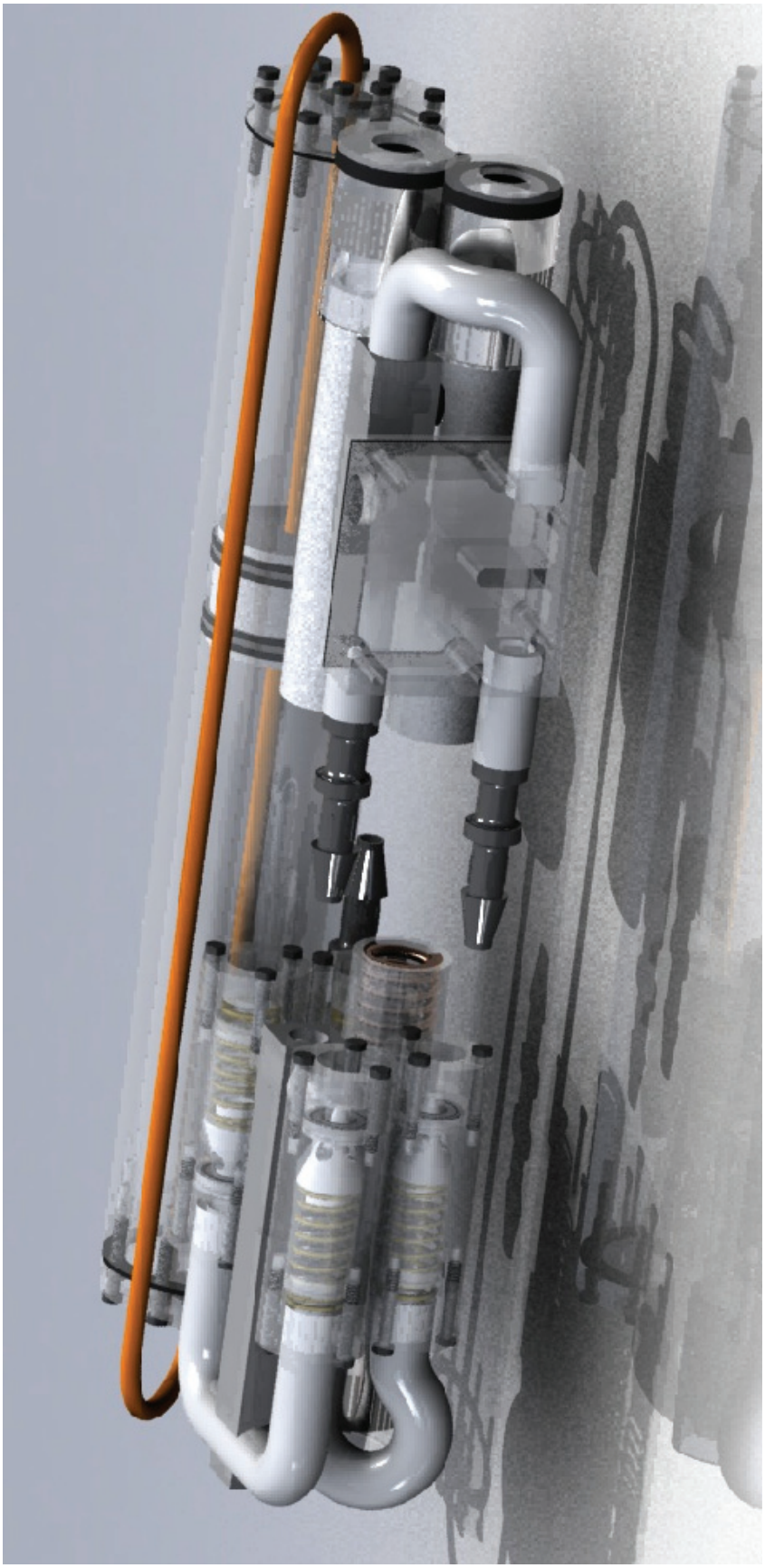

Full Assembly

Manufacturing Drawings

Full sized drawings are available on the documentation CD. The drawings in this document have been reduced in size for brevity.

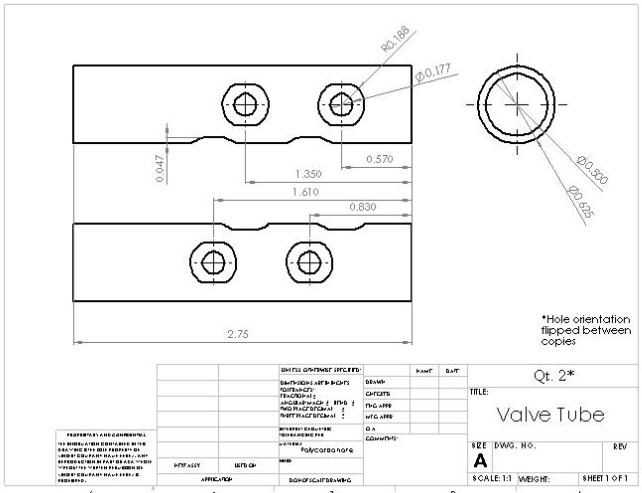

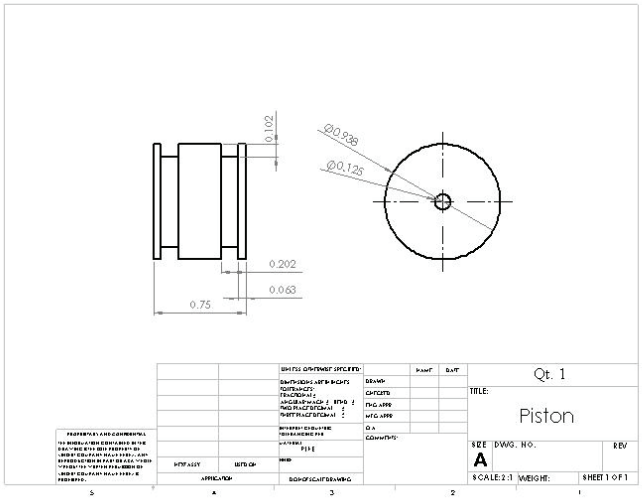

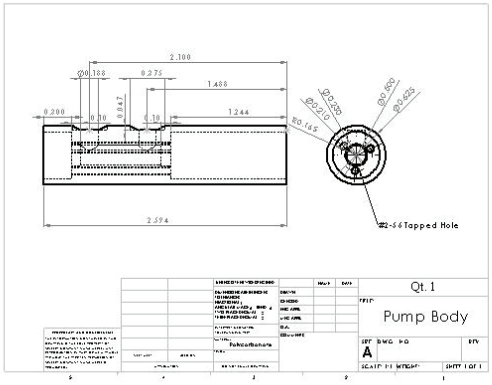
2.100
Ø0.188
0.275
1.488
0.200
0.70
0.10
1.244
Ø0.350
Ø0.270
Ø0.500
Ø0.425
R0.145
2.594
#2-56 Tapped Hole
Qt. 1
Pump Body
A

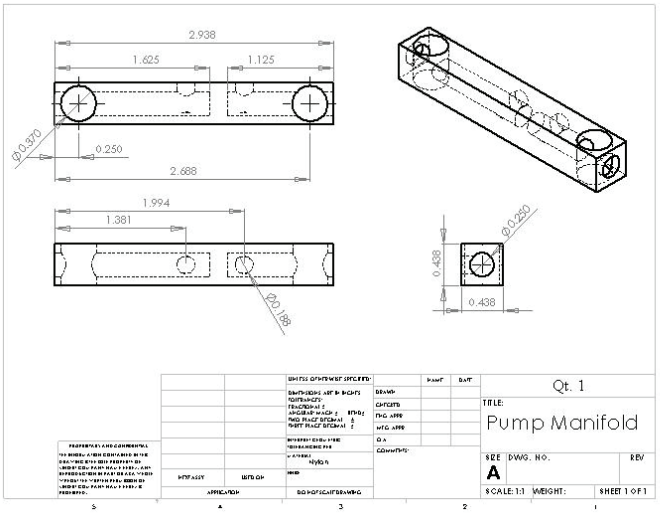
2.938
1.625
1.125
Ø0.370
0.250
2.688
1.994
1.381
Ø0.188
Ø0.250
0.438
0.438
Qt. 1
TITLE:
Pump Manifold
SIZE
A
DWG. NO.
REV
SCALE: 1:1
WEIGHT:
SHEET 1 OF 1

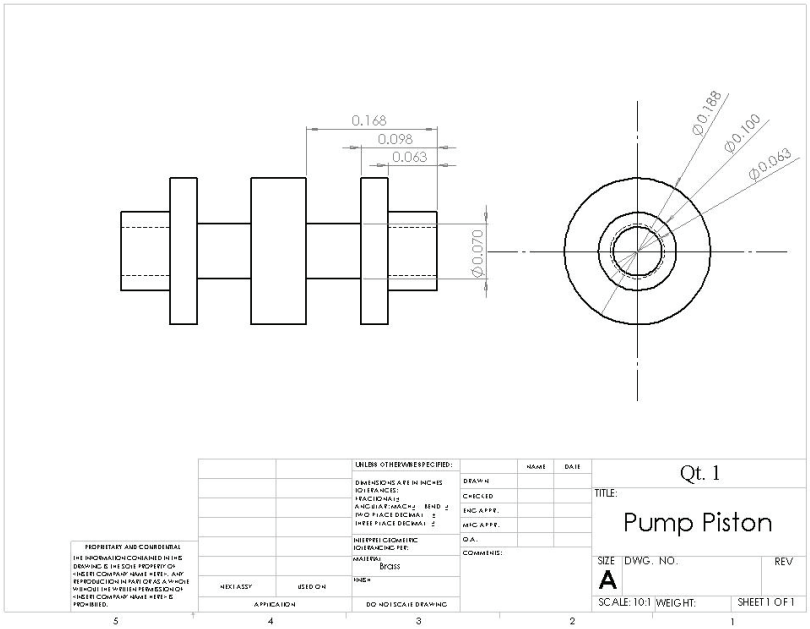
0.168
0.098
0.063
Ø0.070
Ø0.188
Ø0.100
Ø0.063
Qt. 1
TITLE:
Pump Piston
SIZE
A
DWG. NO.
REV
SCALE: 10:1
WEIGHT:
SHEET 1 OF 1

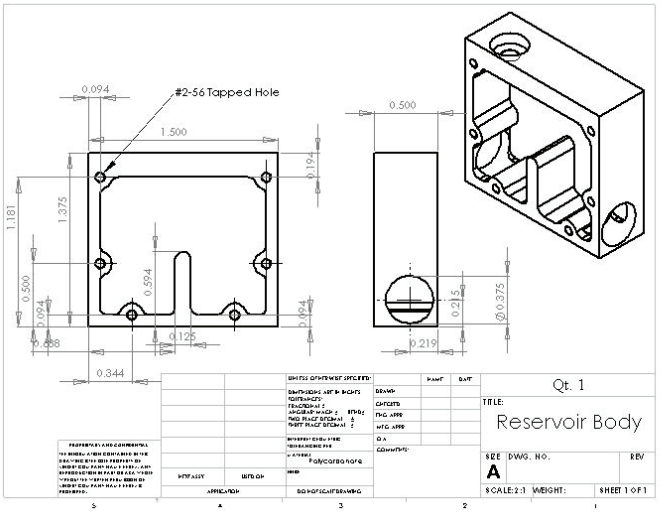
0.094
#2-56 Tapped Hole
1.500
0.194
1.181
1.375
0.500
0.594
0.094
0.094
0.688
0.125
0.344
0.500
0.215
Ø0.375
0.219
Qt. 1
TITLE:
Reservoir Body
SIZE
A
DWG. NO.
REV
SCALE: 2:1
WEIGHT:
SHEET 1 OF 1

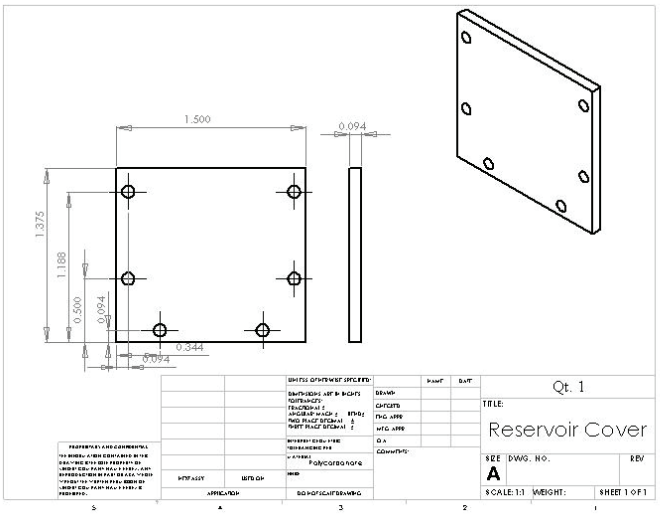
1.500
0.094
1.375
1.188
0.500
0.094
0.344
0.094
Qt. 1
TITLE:
Reservoir Cover
SIZE
A
DWG. NO.
REV
SCALE: 1:1
WEIGHT:
SHEET 1 OF 1

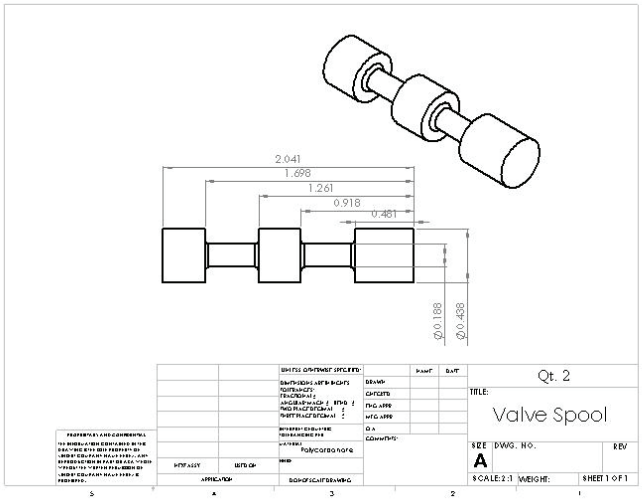
2.041
1.698
1.261
0.918
0.481
Ø0.188
Ø0.438
Qt. 2
TITLE:
Valve Spool
SIZE
A
DWG. NO.
REV
SCALE: 2:1
WEIGHT:
SHEET 1 OF 1

Component Information

BPW24R

Vishay Semiconductors

Silicon PIN Photodiode, RoHS Compliant

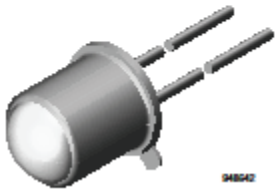

FEATURES

- Package type: leaded
- Package form: TO-18
- Dimensions (in mm): Ø 4.7
- Radiant sensitive area (in mm²): 0.78
- High photo sensitivity
- High radiant sensitivity
- Suitable for visible and near infrared radiation
- Fast response times
- Angle of half sensitivity: $\varphi = \pm 12°$
- Hermetically sealed package
- Cathode connected to package
- Central chip alignment
- Lead (Pb)-free component in accordance with RoHS 2002/95/EC and WEEE 2002/96/EC

APPLICATIONS

- High speed photo detector

DESCRIPTION

BPW24R is a high sensitive silicon planar photodiode in a standard TO-18 hermetically sealed metal case with a glass lens.
A precise alignment of the chip gives a good coincidence of mechanical and optical axes. The device features a low capacitance and high speed even at low supply voltages.

PRODUCT SUMMARY

COMPONENT	I_{ra} (µA)	φ (deg)	$\lambda_{0.5}$ (nm)
BPW24R	60	± 12	600 to 1050

Note
Test condition see table "Basic Characteristics"

ORDERING INFORMATION

ORDERING CODE	PACKAGING	REMARKS	PACKAGE FORM
BPW24R	Bulk	MOQ: 1000 pcs, 1000 pcs/bulk	TO-18

Note
MOQ: minimum order quantity

ABSOLUTE MAXIMUM RATINGS

PARAMETER	TEST CONDITION	SYMBOL	VALUE	UNIT
Reverse voltage		V_R	60	V
Power dissipation	$T_{amb} \leq 25$ °C	P_V	210	mW
Junction temperature		T_j	125	°C
Operating temperature range		T_{amb}	- 40 to + 125	°C
Storage temperature range		T_{stg}	- 40 to + 125	°C
Soldering temperature	$t \leq 5$ s	T_{sd}	260	°C
Thermal resistance junction/ambient	Connected with Cu wire, 0.14 mm²	R_{thJA}	350	K/W

Note
T_{amb} = 25 °C, unless otherwise specified

ANALOG DEVICES

Switched-Capacitor Voltage Inverter with Shutdown

ADM8828/ADM8829

FEATURES

Inverts Input Supply Voltage
99% Voltage Conversion Efficiency
25 mA Output Current
Shutdown Function
Requires Only Two Capacitors
1 μF Capacitors
18 Ω Output Resistance
+1.5 V to +5.5 V Input Range
600 μA Quiescent Current
20 nA Shutdown Current (ADM8828)

APPLICATIONS

Handheld Instruments
LCD Panels
Cellular Phones
PDAs
Remote Data Acquisition
Op Amp Power Supplies

FUNCTIONAL BLOCK DIAGRAMS

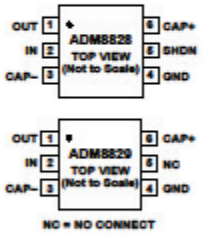

GENERAL DESCRIPTION

The ADM8828/ADM8829 is a charge-pump voltage inverter which may be used to generate a negative supply from a positive input. Input voltages ranging from +1.5 V to +5.5 V can be inverted into a negative –1.5 V to –5.5 V output supply. This inverting scheme is ideal for generating a negative rail in single power-supply systems. Only two small external capacitors are needed for the charge pump. Output currents up to 25 mA with greater than 99% efficiency are achievable.

The ADM8828 also features a low power shutdown (SHDN) pin. This can be used to disable the device and reduce the quiescent current to 20 nA.

The ADM8828/ADM8829 is available in a 6-lead SOT-23 package.

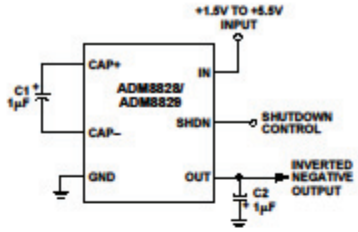

Figure 1. Typical Circuit Configuration

REV. A

One Technology Way, P.O. Box 9106, Norwood, MA 02062-9106, U.S.A.
Tel: 781/329-4700 World Wide Web Site: http://www.analog.com
Fax: 781/326-8703

August 2000

National Semiconductor

LMC6484
CMOS Quad Rail-to-Rail Input and Output Operational Amplifier

General Description

The LMC6484 provides a common-mode range that extends to both supply rails. This rail-to-rail performance combined with excellent accuracy, due to a high CMRR, makes it unique among rail-to-rail input amplifiers.

It is ideal for systems, such as data acquisition, that require a large input signal range. The LMC6484 is also an excellent upgrade for circuits using limited common-mode range amplifiers such as the TLC274 and TLC279.

Maximum dynamic signal range is assured in low voltage and single supply systems by the LMC6484's rail-to-rail output swing. The LMC6484's rail-to-rail output swing is guaranteed for loads down to 600Ω.

Guaranteed low voltage characteristics and low power dissipation make the LMC6484 especially well-suited for battery-operated systems.

See the LMC6482 data sheet for a Dual CMOS operational amplifier with these same features.

Features

(Typical unless otherwise noted)

- Rail-to-Rail Input Common-Mode Voltage Range (Guaranteed Over Temperature)
- Rail-to-Rail Output Swing (within 20 mV of supply rail, 100 kΩ load)
- Guaranteed 3V, 5V and 15V Performance
- Excellent CMRR and PSRR: 82 dB
- Ultra Low Input Current: 20 fA
- High Voltage Gain (R_L = 500 kΩ): 130 dB
- Specified for 2 kΩ and 600Ω loads

Applications

- Data Acquisition Systems
- Transducer Amplifiers
- Hand-held Analytic Instruments
- Medical Instrumentation
- Active Filter, Peak Detector, Sample and Hold, pH Meter, Current Source
- Improved Replacement for TLC274, TLC279

3V Single Supply Buffer Circuit

Rail-to-Rail Input

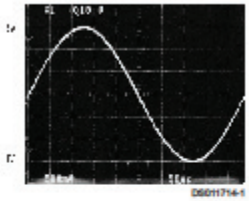

DS011714-1

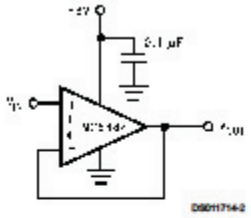

DS011714-2

Rail-to-Rail Output

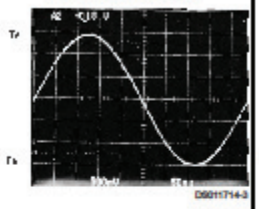

DS011714-3

SLLS047L – FEBRUARY 1989 – REVISED MARCH 2004

- Meets or Exceeds TIA/EIA-232-F and ITU Recommendation V.28
- Operates From a Single 5-V Power Supply With 1.0-μF Charge-Pump Capacitors
- Operates Up To 120 kbit/s
- Two Drivers and Two Receivers
- ±30-V Input Levels
- Low Supply Current . . . 8 mA Typical
- ESD Protection Exceeds JESD 22
  - 2000-V Human-Body Model (A114-A)
- Upgrade With Improved ESD (15-kV HBM) and 0.1-μF Charge-Pump Capacitors is Available With the MAX202
- Applications
  - TIA/EIA-232-F, Battery-Powered Systems, Terminals, Modems, and Computers

MAX232 . . . D, DW, N, OR NS PACKAGE
MAX232I . . . D, DW, OR N PACKAGE
(TOP VIEW)

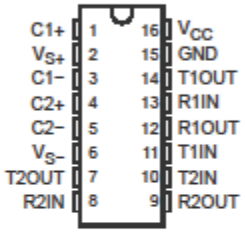

description/ordering information

The MAX232 is a dual driver/receiver that includes a capacitive voltage generator to supply TIA/EIA-232-F voltage levels from a single 5-V supply. Each receiver converts TIA/EIA-232-F inputs to 5-V TTL/CMOS levels. These receivers have a typical threshold of 1.3 V, a typical hysteresis of 0.5 V, and can accept ±30-V inputs. Each driver converts TTL/CMOS input levels into TIA/EIA-232-F levels. The driver, receiver, and voltage-generator functions are available as cells in the Texas Instruments LinASIC™ library.

ORDERING INFORMATION

T_A	PACKAGE†		ORDERABLE PART NUMBER	TOP-SIDE MARKING
0°C to 70°C	PDIP (N)	Tube of 25	MAX232N	MAX232N
	SOIC (D)	Tube of 40	MAX232D	MAX232
		Reel of 2500	MAX232DR	
	SOIC (DW)	Tube of 40	MAX232DW	MAX232
		Reel of 2000	MAX232DWR	
	SOP (NS)	Reel of 2000	MAX232NSR	MAX232
−40°C to 85°C	PDIP (N)	Tube of 25	MAX232IN	MAX232IN
	SOIC (D)	Tube of 40	MAX232ID	MAX232I
		Reel of 2500	MAX232IDR	
	SOIC (DW)	Tube of 40	MAX232IDW	MAX232I
		Reel of 2000	MAX232IDWR	

† Package drawings, standard packing quantities, thermal data, symbolization, and PCB design guidelines are available at www.ti.com/sc/package.

GaAlAs-Lumineszenzdioden (880 nm)
GaAlAs Infrared Emitters (880 nm)
Lead (Pb) Free Product - RoHS Compliant

SFH 480, SFH 481, SFH 482

SFH 480

SFH 481:
Nicht für Neuentwicklungen
Not for new designs

SFH 482

Wesentliche Merkmale

- Typische Peakwellenlänge 880nm
- Hermetisch dichtes Metallgehäuse
- SFH 480: Gehäusegleich mit SFH 216
- SFH 481: Gehäusegleich mit BPX 43
- SFH 482: Gehäusegleich mit BPX 38, BPX 65

Features

- Typical peak wavelength 880nm
- Hermetically sealed package
- SFH 480: Same package as SFH 216
- SFH 481: Same package as BPX 43
- SFH 482: Same package as BPX 38, BPX 65

Anwendungen

- Lichtschranken für Gleich- und Wechsellichtbetrieb
- IR-Gerätefernsteuerungen
- Sensorik
- Lichtgitter

Applications

- Photointerrupters
- IR remote control
- Sensor technology
- Light curtains

Wiring Diagram

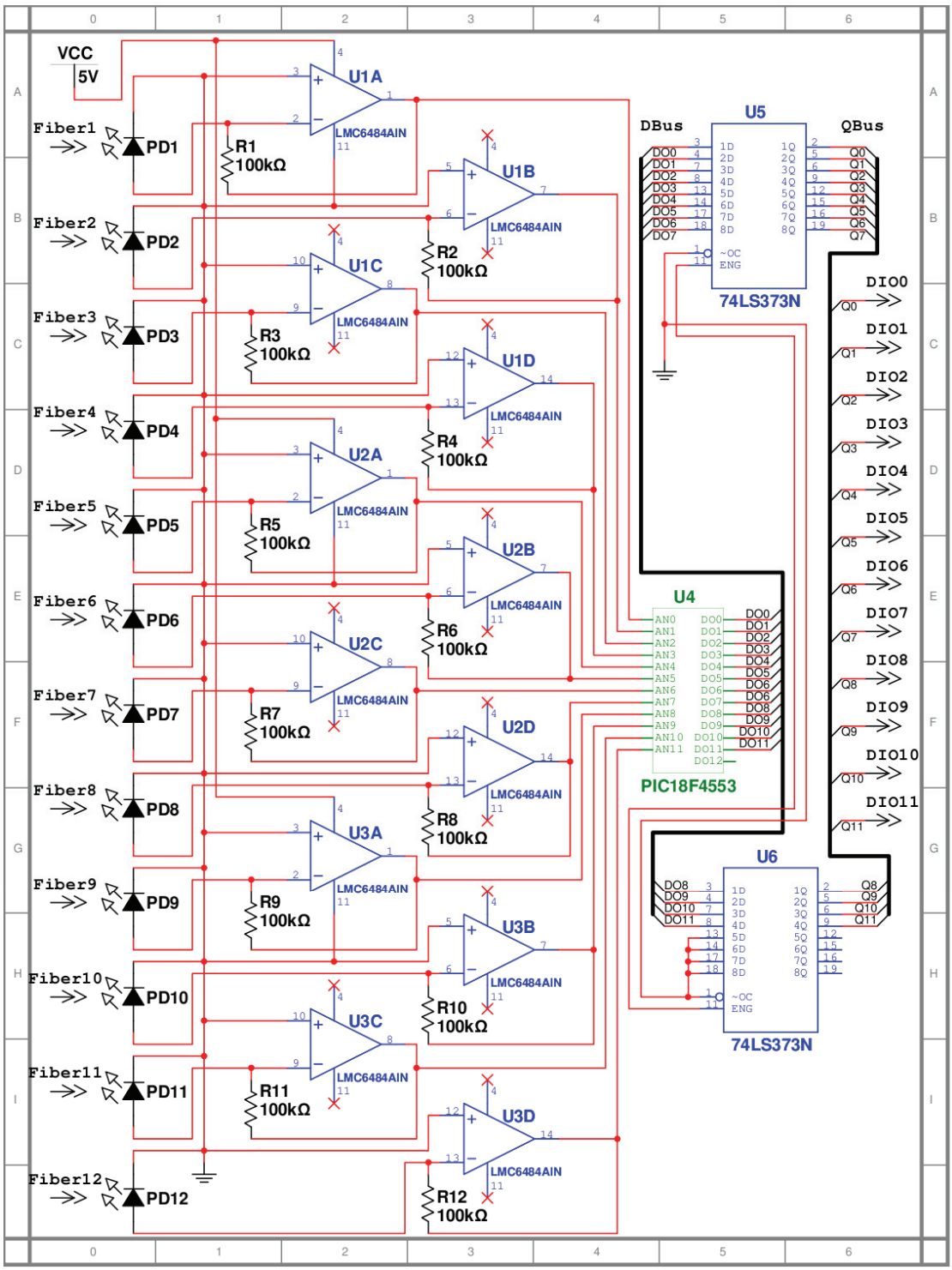

LabVIEW

Prototype Stepper Code

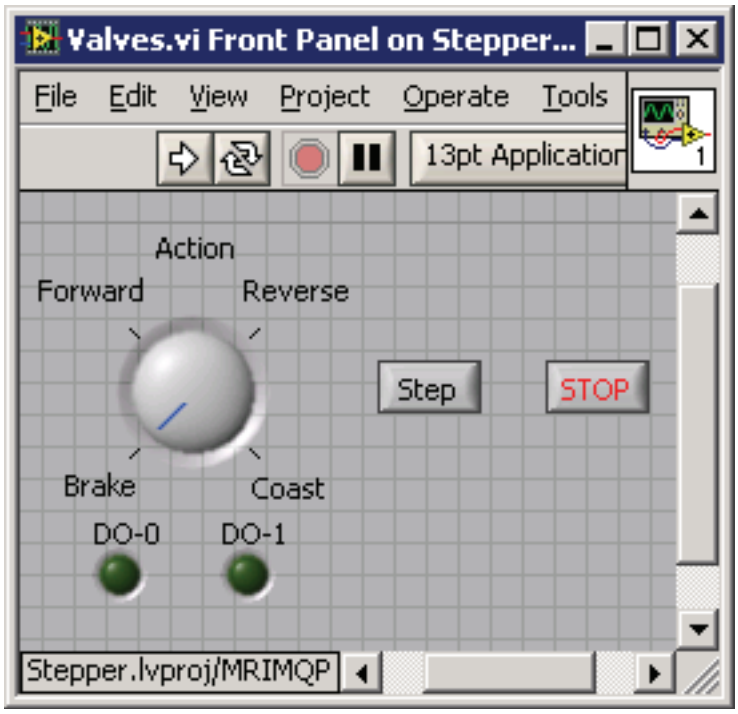

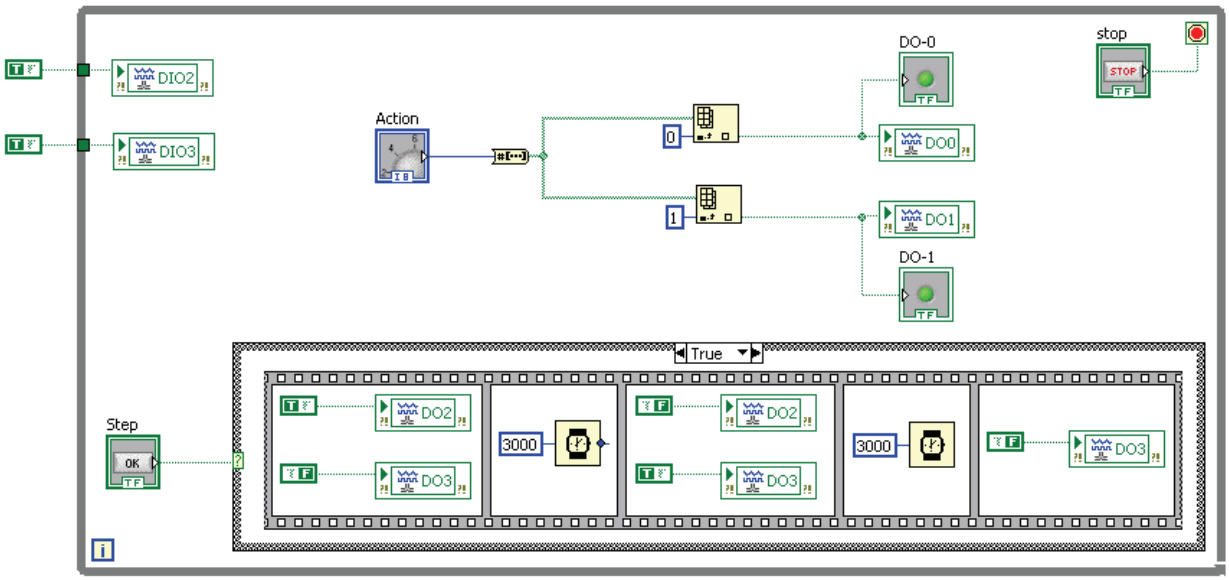

Final Stepper Code

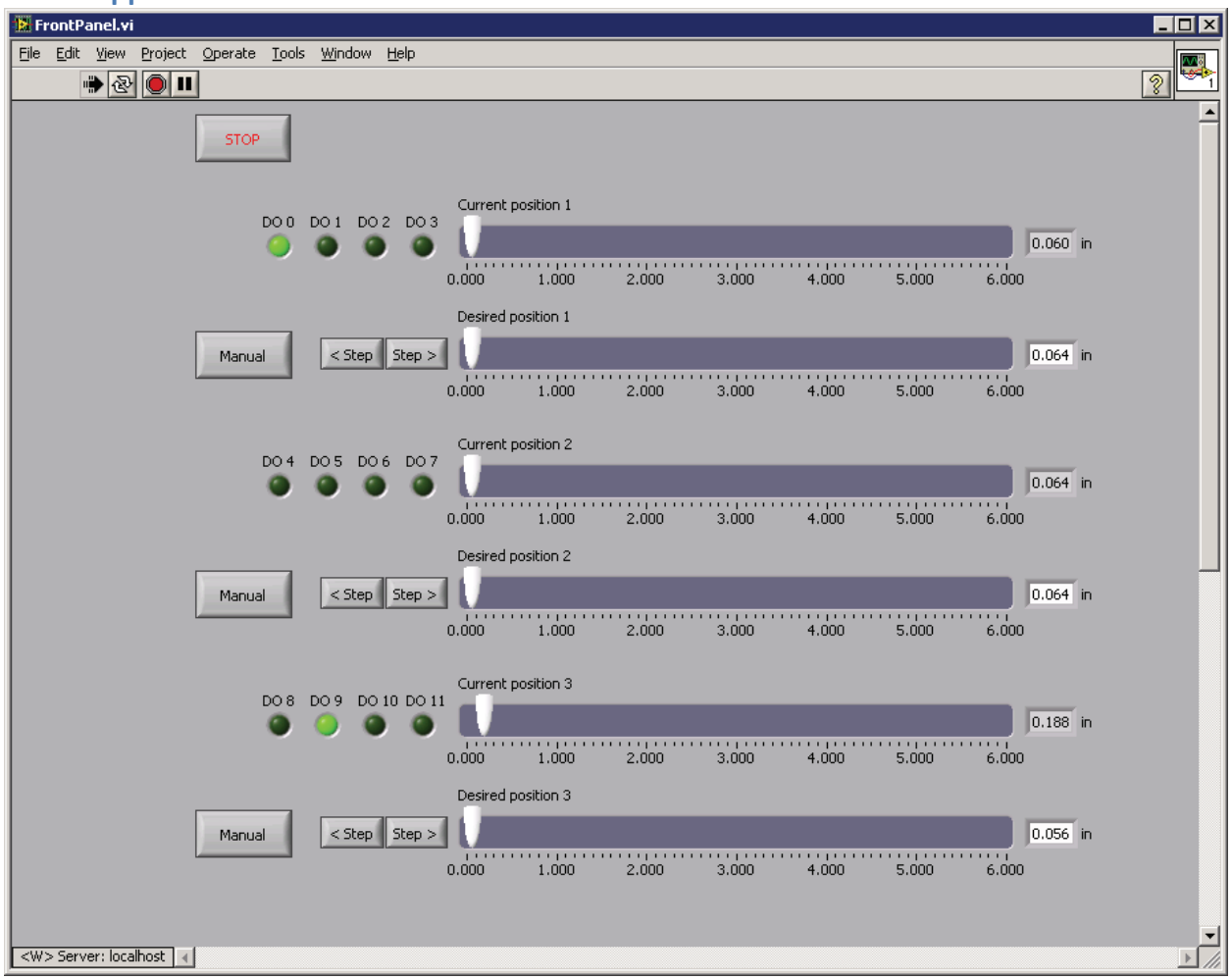

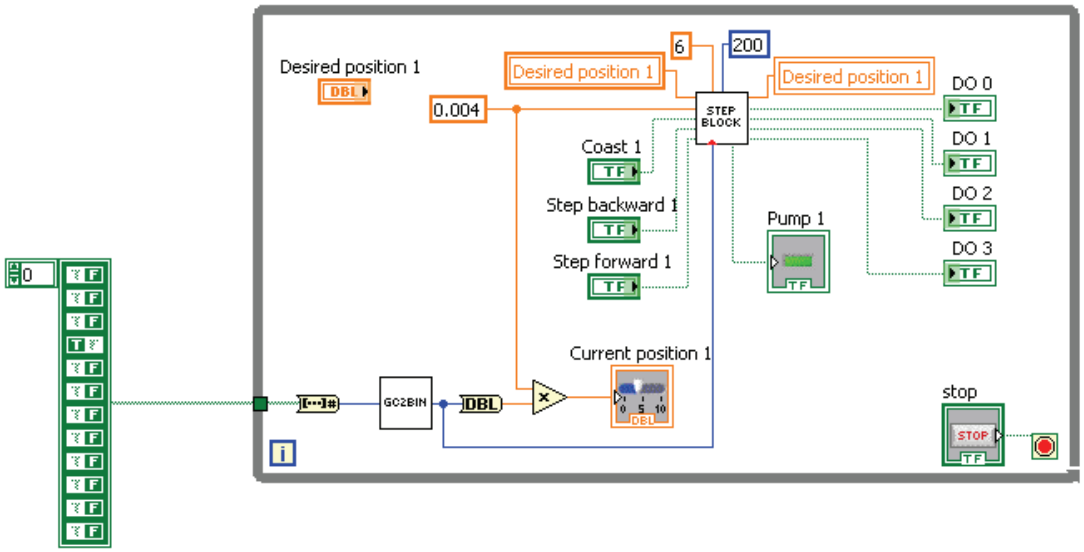

Final Sub-VIs

Stepper

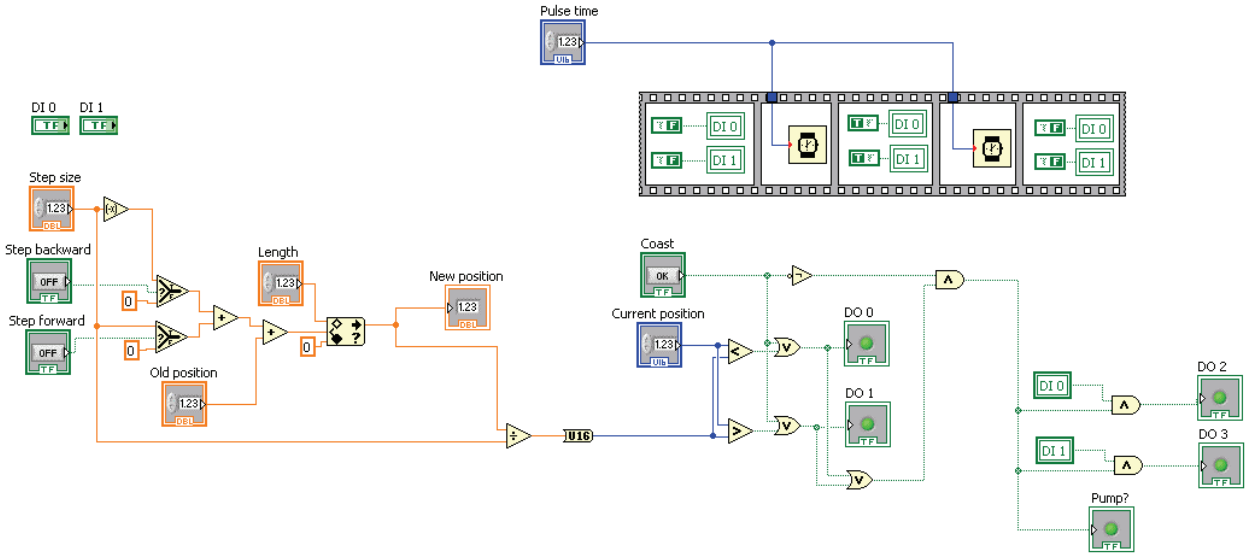

graycode2binary

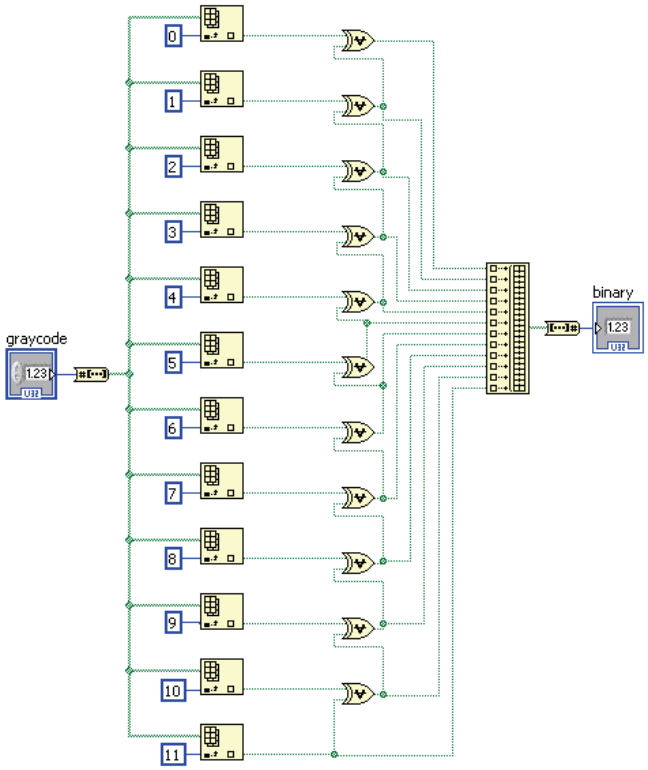

PIC Code

Mrimqp.c

```
/**
 * MRI MQP
 *
 * @author Andrew Smith (asmith@wpi.edu)
 */

#include <p18f4553.h>
#include "mrimqp.h"
#include <stdlib.h>

#include <delays.h>

#pragma config FOSC = INTOSC_HS
#pragma config WDT = OFF
#pragma config PWRT = OFF
#pragma config LVP = OFF

void main(void) {

        //unsigned char a0, a1, a2, a3;
        unsigned short adcVal;

        init();

        D0val = DON;
        D1val = DOFF;
        D2val = DON;
        D3val = DOFF;

        while(1) {
                //ADCON0 |= 0x00;
                Delay10KTCYx(25);
                ADCON0bits.GO = 1;
                while(ADCON0bits.NOT_DONE);
                adcVal = (unsigned short)(ADRESH) << 8 | ADRESL;
                D0val = (adcVal & 0x0001) ? DON : DOFF;
                D1val = (adcVal & 0x0002) ? DON : DOFF;
                D2val = (adcVal & 0x0004) ? DON : DOFF;
                D3val = (adcVal & 0x0008) ? DON : DOFF;
                D4val = (adcVal & 0x0010) ? DON : DOFF;
                D5val = (adcVal & 0x0020) ? DON : DOFF;
                D6val = (adcVal & 0x0040) ? DON : DOFF;
                D7val = (adcVal & 0x0080) ? DON : DOFF;
                D8val = (adcVal & 0x0100) ? DON : DOFF;
                D9val = (adcVal & 0x0200) ? DON : DOFF;
                D10val = (adcVal & 0x0400) ? DON : DOFF;
                D11val = (adcVal & 0x0800) ? DON : DOFF;
        }
}

/* Initialization */
void init(void) {
        /* Use internal oscillator */
        OSCCONbits.SCS1 = 1;

        /* Turn off the Watch-Dog Timer */
        WDTCONbits.SWDTEN = 0;

        PORTA = 0x00;
        ADCON0 = 0x01;
        ADCON1 = 0x0E;
        ADCON2 = 0xBF;
        CMCON = 0x07;
```

```
        D0dir = OUTPUT;
        D1dir = OUTPUT;
        D2dir = OUTPUT;
        D3dir = OUTPUT;
        D4dir = OUTPUT;
        D5dir = OUTPUT;
        D6dir = OUTPUT;
        D7dir = OUTPUT;
        D8dir = OUTPUT;
        D9dir = OUTPUT;
        D10dir = OUTPUT;
        D11dir = OUTPUT;

        /*A0dir = INPUT;
        A1dir = INPUT;
        A2dir = INPUT;
        A3dir = INPUT;*/

}

/* One microsecond delay */
void delay1us(void) {
        Nop();
        return;
}
```

Mrimqp.h

```
#ifndef __MRIMQP_H
#define __MRIMQP_H

#define OUTPUT 0
#define INPUT  1
#define DOFF   0
#define DON            1

#define NUM_PINS 4

#define D0dir TRISAbits.TRISA3
#define D0val LATAbits.LATA3
#define D1dir TRISAbits.TRISA2
#define D1val LATAbits.LATA2
#define D2dir TRISAbits.TRISA1
#define D2val LATAbits.LATA1
#define D3dir TRISDbits.TRISD1
#define D3val LATDbits.LATD1
#define D4dir TRISEbits.TRISE1
#define D4val LATEbits.LATE1
#define D5dir TRISEbits.TRISE0
#define D5val LATEbits.LATE0
#define D6dir TRISDbits.TRISD0
#define D6val LATDbits.LATD0
#define D7dir TRISCbits.TRISC0
#define D7val LATCbits.LATC0
#define D8dir TRISCbits.TRISC1
#define D8val LATCbits.LATC1
#define D9dir TRISCbits.TRISC2
#define D9val LATCbits.LATC2
#define D10dir TRISAbits.TRISA4
#define D10val LATAbits.LATA4
#define D11dir TRISAbits.TRISA5
#define D11val LATAbits.LATA5

void init(void);
void delay1us(void);

#endif
```